Ref
FAA-93-10

DOT/FAA/CT-93/78
DOT-VNTSC-FAA-93-10

FAA Technical Center
Atlantic City International Airport,
N.J. 08405

Full-Scale Testing and Analysis of Curved Aircraft Fuselage Panels

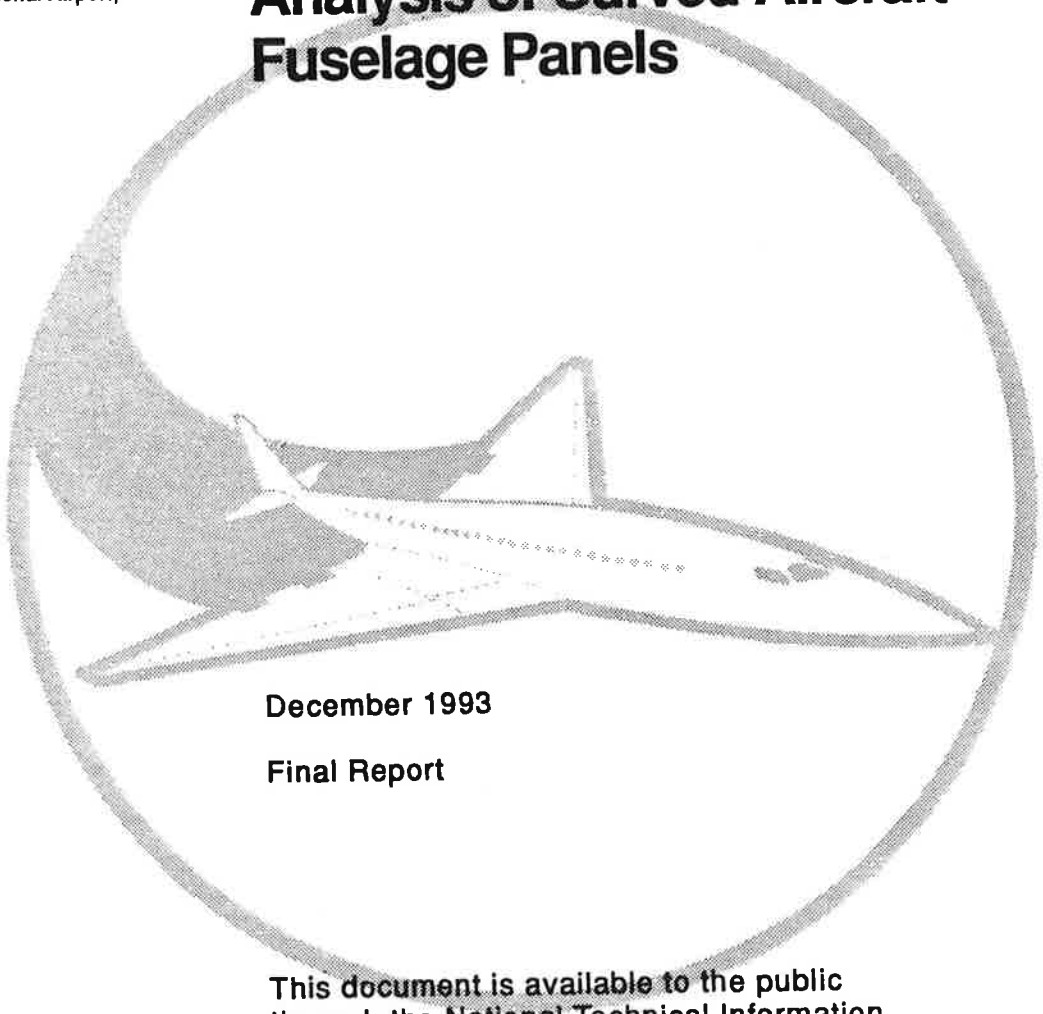

December 1993

Final Report

U.S. Department of Transportation
Federal Aviation Administration

REPORT DOCUMENTATION PAGE

Form Approved
OMB No. 0704-0188

1. AGENCY USE ONLY (Leave blank)

2. REPORT DATE
December 1993

3. REPORT TYPE AND DATES COVERED
Final Report
May 1991 - March 1992

4. TITLE AND SUBTITLE
Full-Scale Testing and Analysis of Curved Aircraft Fuselage Panels

5. FUNDING NUMBERS
FA3H2/A3128
DTRS-57-89-D-00009

6. AUTHOR(S)
G. Samavedam, D. Hoadley, D. Thomson

7. PERFORMING ORGANIZATION NAME(S) AND ADDRESS(ES)
Foster-Miller, Inc. *
350 Second Avenue
Waltham, MA 02154-1196

8. PERFORMING ORGANIZATION REPORT NUMBER
DOT-VNTSC-FAA-93-10

9. SPONSORING/MONITORING AGENCY NAME(S) AND ADDRESS(ES)
U.S. Department of Transportation
Federal Aviation Administration Technical Center
Atlantic City International Airport, NJ 08405

10. SPONSORING/MONITORING AGENCY REPORT NUMBER
DOT/FAA/CT-93/78

11. SUPPLEMENTARY NOTES
* under contract to: U.S. Department of Transportation
Volpe National Transportation Systems Center
Kendall Square
Cambridge, MA 02142-1093

12a. DISTRIBUTION/AVAILABILITY STATEMENT
This document is available to the public through the National Technical Information Service, Springfield, VA 22161

12b. DISTRIBUTION CODE

13. ABSTRACT (Maximum 200 words)

This report presents data on (i) residual strength of aircraft panels containing Multiple-Site Damage (MSD) in lap splices, and (ii) fatigue strength of panels subjected to cyclic pressure loading. The testing was conducted using the dedicated Aging Aircraft Test Facility previously built in the Foster-Miller laboratory. A previous report describes the work in the first phase involving the design and operation of the facility and the test data generated on residual strength of panels with longitudinal midday skin cracks.

In the Phase II work presented here, several residual strength tests were conducted to develop a relationship between failure pressure and the lead crack length in the critical upper rivet line of the lap joint. In some of the panels multiple-site damage was also built in the rivet line during fabrication. The reduction in the residual strength due to MSD has been experimentally quantified. Conditions of crack arrest at tear straps and panel flapping were also investigated.

Fatigue testing of the panel, with no initial damage in the lap splice except an unbonded lap joint area, was conducted to investigate the crack initiation at multiple sites, crack growth rates and eventual linkup of the ligaments and fracture failure. The ultimate life of the panel, and the damage in critical upper and lower skin rivet rows was determined. Conclusions of practical interest were drawn from the test data.

14. SUBJECT TERMS
Aging Aircraft, Multiple-Site Damage, Fuselage Fracture, Fatigue, Lap Splice, Residual Strength

15. NUMBER OF PAGES
58

16. PRICE CODE

17. SECURITY CLASSIFICATION OF REPORT	18. SECURITY CLASSIFICATION OF THIS PAGE	19. SECURITY CLASSIFICATION OF ABSTRACT	20. LIMITATION OF ABSTRACT
Unclassified	Unclassified	Unclassified	

PREFACE

This report presents data on (i) residual strength of aircraft panels containing Multiple-Site Damage (MSD) in lap splices, and (ii) fatigue strength of panels subjected to cyclic pressure loading. The testing was conducted using the dedicated Aging Aircraft Test Facility previously built in the Foster-Miller laboratory. A previous report describes the work in the first phase involving the design and operation of the facility and the test data generated on residual strength of panels with longitudinal midbay skin cracks.

In the Phase II work presented here, several residual strength tests were conducted to develop a relationship between failure pressure and the lead crack length in the critical upper rivet line of the lap joint. In some of the panels, Multiple-Site Damage was also built in the rivet line during fabrication. The reduction in the residual strength due to MSD has been experimentally quantified. Conditions of crack arrest at tear straps and panel flapping were also investigated.

The report was prepared for the Volpe National Transportation Systems Center (VNTSC) in support of the Federal Aviation Administration (FAA) Technical Center under contract DTRS-57-89-D-0009.

Special thanks are due to Messrs Tom Swift and David Broek for their technical inputs.

The extensive work performed by John McHatton in the test operations is acknowledged. Thanks also to Mike Winter of ECAT for support given in the panel fabrication.

METRIC/ENGLISH CONVERSION FACTORS

ENGLISH TO METRIC

LENGTH (APPROXIMATE)

1 inch (in) = 2.5 centimeters (cm)
1 foot (ft) = 30 centimeters (cm)
1 yard (yd) = 0.9 meter (m)
1 mile (mi) = 1.6 kilometers (km)

AREA (APPROXIMATE)

1 square inch (sq in, in^2) = 6.5 square centimeters (cm^2)
1 square foot (sq ft, ft^2) = 0.09 square meter (m_2)
1 square yard (sq yd, yd^2) = 0.8 square meter (m^2)
1 square mile (sq mi, mi^2) = 2.6 square kilometers (km^2)
1 acre = 0.4 hectares (he) = 4,000 square meters (m^2)

MASS - WEIGHT (APPROXIMATE)

1 ounce (oz) = 28 grams (gr)
1 pound (lb) = .45 kilogram (kg)
1 short ton = 2,000 pounds (lb) = 0.9 tonne (t)

VOLUME (APPROXIMATE)

1 teaspoon (tsp) = 5 milliliters (ml)
1 tablespoon (tbsp) = 15 milliliters (ml)
1 fluid ounce (fl oz) = 30 milliliters (ml)
1 cup (c) = 0.24 liter (1)
1 pint (pt) = 0.47 liter (1)
1 quart (qt) = 0.96 liter (1)
1 gallon (gal) = 3.8 liters (1)
1 cubic foot (cu ft, ft^3) = 0.03 cubic meter (m^3)
1 cubic yard (cu yd, yd^3) = 0.76 cubic meter (m^3)

TEMPERATURE (EXACT)

$[(x-32)(5/9)]\ ^{o}F = y\ ^{o}C$

METRIC TO ENGLISH

LENGTH (APPROXIMATE)

1 millimeter (mm) = 0.04 inch (in)
1 centimeter (cm) = 0.4 inch (in)
1 meter (m) = 3.3 feet (ft)
1 meter (m) = 1.1 yards (yd)
1 kilometer (km) = 0.6 mile (mi)

AREA (APPROXIMATE)

1 square centimeter (cm^2) = 0.16 square inch (sq in, in^2)
1 square meter (m^2) = 1.2 square yeards (sq yd, yd^2)
1 square kilometer (km^2) = 0.4 square mile (sq mi, mi^2)
1 hectare (he) = 10,000 square meters (m^2) = 2.5 acres

MASS - WEIGHT (APPROXIMATE)

1 gram (gr) = 0.036 ounce (oz)
1 kilogram (kg) = 2.2 pounds (lb)
1 tonne (t) = 1,000 kilograms (kg) = 1.1 short tons

VOLUME (APPROXIMATE)

1 milliliters (ml) = 0.03 fluid ounce (fl oz)
1 liter (1) = 2.1 pints (pt)
1 liter (1) = 1.06 quarts (qt)
1 liter (1) = 0.26 gallon (gal)
1 cubic meter (m^3) = 36 cubic feet (cu ft, ft^3)
1 cubic meter (m^3) = 1.3 cubic yards (cu yd, yd^3)

TEMPERATURE (EXACT)

$[(9/5)\ y + 32]\ ^{o}C = x\ ^{o}F$

QUICK INCH-CENTIMETER LENGTH CONVERSION

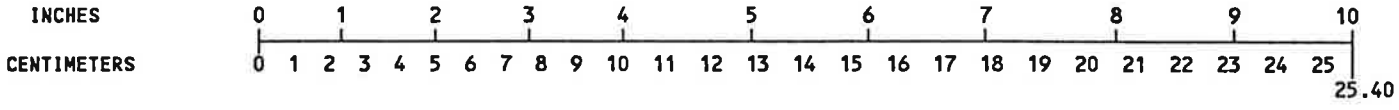

QUICK FAHRENHEIT-CELSIUS TEMPERATURE CONVERSION

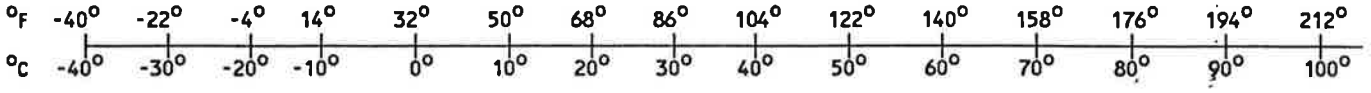

For more exact and or other conversion factors, see NBS Miscellaneous Publication 286, Units of Weights and Measures. Price $2.50. SD Catalog No. C13 10286.

TABLE OF CONTENTS

TABLE OF CONTENTS (Continued)

LIST OF ILLUSTRATIONS

LIST OF ILLUSTRATIONS

LIST OF TABLES

Table **Page**

1. INTRODUCTION

This document is the Draft Final Technical Report on OMNI Technical Task Directive No. VA 1027 titled, "Full-Scale Testing and Analysis of Fuselage Panels." This effort is a major part of the Federal Aviation Administration's (FAA's) Aging Aircraft Research Program and is a follow-on from OMNI Technical Task Directive No. VA9007, (Phase I) the results of which were reported in May 1991 (1). The specific activities described in this report include panel design, fabrication and fatigue and fracture testing of full-scale curved fuselage panels under static and cyclic pressurization loads. Also described is the development of an analytical model for the riveted lap joint of a curved stiffened fuselage panel.

1.1 Background (Phase I Summary)

The objectives of the Phase I program were: design and fabricate a full-scale curved fuselage test facility, design representative fuselage panel test specimens, conduct shakedown testing to evaluate facility performance, evaluate skin cracks through fracture tests, and develop an analytical fracture model for a curved stiffened fuselage panel.

Fuselage panel configurations were designed to represent critical construction features of the older vintage commercial aircraft. These panels were designed to minimize the effects of boundaries and attachment. They were also designed to allow the incorporation, during manufacture, of specific defects like Multiple Site Damage (MSD), disbonding, long skin cracks, repairs, or simulated corrosion.

A total of nine tests were conducted. Eight were residual strength tests and one was a fatigue test. Residual strength tests performed were on panels with midbay cracks of 16, 24, and 36 in. in length and no MSD. These tests were conducted to develop a relationship between the panel residual strength and the length of the skin lead cracks. Further, the direction of crack propagation provided a measure of the performance of the panel frames and tear straps. Two other tests of residual strength simulated a lead crack of about 12.4 in. in the panel lap joint upper rivet row with and without the presence of MSD beyond the lead crack tips. These tests indicated a potentially significant residual strength reduction due to MSD as has been theorized by Swift (2) and others. However, further testing to confirm this result was not conducted under this program.

In the fatigue test, a panel with an unbonded lap joint and rivet hole crack initiation notches was cyclically loaded. This test was conducted at a maximum pressure of 150 percent of typical fuselage operational pressure to accelerate testing and to evaluate the capabilities of the test facility.

Throughout the program, extensive analyses were performed in support of the panel design and performance evaluation. Analytical techniques were used to predict the fracture behavior of curved stiffened panels with midbay skin cracks. In particular, Foster-Miller developed a finite element model using NISA 386 to evaluate stress intensity factors (K_I) for a curved stiffened fuselage structure with skin cracks. Numerical analysis was employed to establish the hoop stress equivalency between the actual fuselage structure and a stiffened flat panel for fatigue testing. A 3-D finite element mesh of an unbonded, riveted lap joint was constructed to determine rivet loads and to study their sensitivity to rivet stiffness. The MSD link-up process in a cracked lap joint was investigated in a preliminary manner using the elastoplastic codes in NISA.

The Phase I program demonstrated that stiffened curved fuselage panels can be economically fabricated and tested to yield stress distributions which are representative of a full-scale aircraft fuselage. The program also demonstrated that the test facility is capable of conducting fracture tests as high as 14.2 psi for failure pressure and fatigue tests as high as 720 cycles per hour in cycling rate. The test results generated a relationship of midbay skin crack length and panel residual strength and an analytical fracture model for a curved stiffened fuselage panel was developed. The program concluded that the likelihood of the skin crack to turn as it propagates could apparently not be predicted.

1.2 Phase II Program Summary

The primary objectives of the Phase II program detailed in this report were to evaluate lap splice cracks through fracture tests, and study MSD initiation and link-up in the lap splice through fatigue tests.

Under the program described in this report, fatigue and residual strength tests were performed to more completely characterize panel performance. Design changes were made to the aircraft panels, based in part on the results of the Phase I tests, to more accurately represent the design details of in-service aircraft. These changes, as well as the differences between the residual strength test panels and the fatigue test panels, are discussed in Section 3.

Seven residual strength tests were conducted to develop a relationship between failure pressure and lead crack length for cracks in the upper rivet line of the lap joint. These tests also compared failure of panels with the same lead crack lengths with and without MSD to quantify the expected strength reductions and to investigate the crack growth paths. A matrix of the tests is presented in Section 2. The complete test results are presented in Section 4.

A high cycle fatigue to failure test was conducted on a panel with no initial mechanical damage. Prior to cycling, several surveys were conducted to measure the strain distribution throughout the panel and, more specifically, across the lap joint. Deflection measurements were also made to quantify panel bulging and to relate this data to the strain measurements. A finite element analysis was made of the stresses and deflections across the lap joint for comparison to the measured data. This panel was then cycled at operational pressure until failure with the progression of panel damage monitored at regular intervals. The results of this testing are discussed in Section 5.

Conclusions and recommendations are presented in Section 6.

2. TEST PROGRAM

2.1 Objectives

Based on the findings of the Phase I program and the evaluation requirements of the FAA, a Phase II testing program was developed. The two primary objectives of this program were as follows:

- Evaluate the residual strength of aircraft panels with long lap splice lead cracks and the presence of Multiple Site Damage (MSD).
- Perform a fundamental study of the phenomenon of MSD initiation in the lap splice under pressure cycle fatigue and the resultant crack propagation leading to link-up and ultimate fracture.

2.2 Test Matrix

To address the defined objectives, a test matrix, shown in Table 1, was developed. Seven residual strength tests and one fatigue test were conducted. The primary goal of the residual strength tests was to address the first objective by quantifying panel residual strength as a function of lead crack length and strength reduction due to MSD. The primary goal of the fatigue test was to address the second objective by creating MSD through fatigue cycling of a panel with no initial mechanical damage. Results of all of the tests are discussed in Sections 4 and 5.

Table 1. Phase II Test Matrix

Panel No.	Test Type	Lap Joint Upper Rivet Row Crack		Number of MSD Rivets on Each Side of Crack	Remarks
		Center Location	Length (in.)		
8	RS	F3	23.36	0	
9	RS	F3	23.36	5	
10	RS	F3	29.36	0	
11	RS	F3	29.36	5	
12	FS	-	-	-	Cycle to Failure
14	RS	F3	35.36	0	
15	RS	F3	35.36	5	
16	RS	F3	23.36	0	Frame broken at F3, S3

RS = Residual Strength
FS = Fatigue Strength
Panel configurations are shown in Section 3.
Panels 13 and 17 were manufactured for FS testing but not tested.

3. PANEL DESIGN

The test panel configurations used for testing described in this report are similar to those used for residual strength and fatigue testing in the previous series (1).

When compared to earlier test panels both residual strength and fatigue panels were changed as follows:

- Tear strap widths are 1.4 in. increasing to 2 in. at the tear strap lap joint where six rivets are used. This compares to 1 in. wide straps and three rivets used previously.
- Bonded lap joint widths are 2.7 in. compared to 3.34 in.
- Stringer ties connecting the frames to the stringers have been added. These replace the angle shear clips which connected the frame to the skins in the previous test panels.

3.1 Residual Strength Panel

The configuration of the residual strength panel (9312001) is shown in Figures 1 and 2. Major panel features are listed in Table 2. The panel has one longitudinal lap splice centered over one of the two center stringers. The splice is bonded and joined by three longitudinal rivet rows. The center rivet row also attaches the stringer to the skin. Tear straps are positioned at and between the frames in the hoop direction. One inch wide longitudinal filler strips are used between the tear straps at the stringer locations to provide a waffle-type configuration. All faying surfaces between the skins at the lap joint and the skins and tear straps and filler strips are adhesively bonded.

The stringers are of fabricated hat-section and the frames are of fabricated z-section. Stringers are rivet-attached to the skin through the hat crown. The base of the stringer is rivet-attached to the frame flange by two universal-head rivets at each intersection. The webs of the stringer are attached to the frame by a U-sectioned stringer tie. All through-skin rivets are 5/32-in. diam, low profile, shear head 100-deg countersunk rivets.

The four edges of the test panel are specially prepared for connection to the test fixture. Twenty-eight fingers, each 4 in. wide, are located along each of the two longitudinal panel sides and 16 fingers, each 3.5 in. wide, are located along each of the two curved ends. Each finger is reinforced by two 0.08-in. thick aluminum reinforcing sheets, one bonded to each side of the skin. Each finger assembly includes a 0.75 in. diam centrally positioned hole.

The selected panel configuration has generic similarities to older commercial airframes currently being operated in the United States. The panel is relatively easy to fabricate and assemble. The panel periphery configuration has been selected to minimize the effects of test fixture attachment. The individual finger design provides a means of in-plane connection of the skin to the fixture. The longitudinal fingers will transmit panel hoop loads to the test rig. These fingers have been designed to provide minimal longitudinal stiffness to the panel. Similarly, the fingers on the two curved ends transmit only longitudinal loads to the rig. Their contribution to panel hoop stiffness is minimal. The panel includes a short section of unstiffened skin immediately inboard of all the load fingers. This section is clear of frames, tear straps, fillers and stringers and is provided as a clear surface for the bearing of the inflatable peripheral seals. Rivet orientation in this region of the lap splice has been reversed to place the countersunk head on

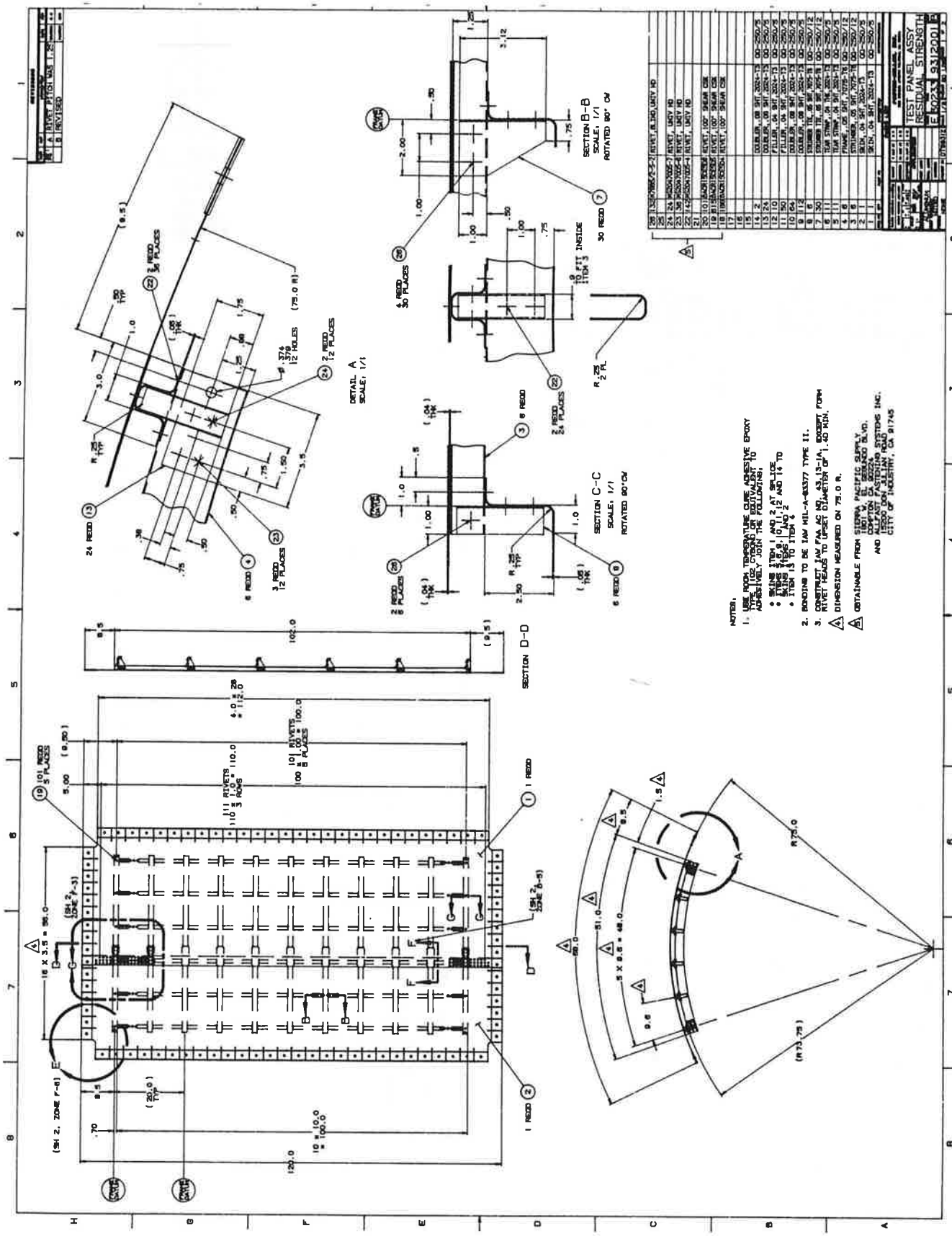

Figure 1. Residual Strength Test Panel

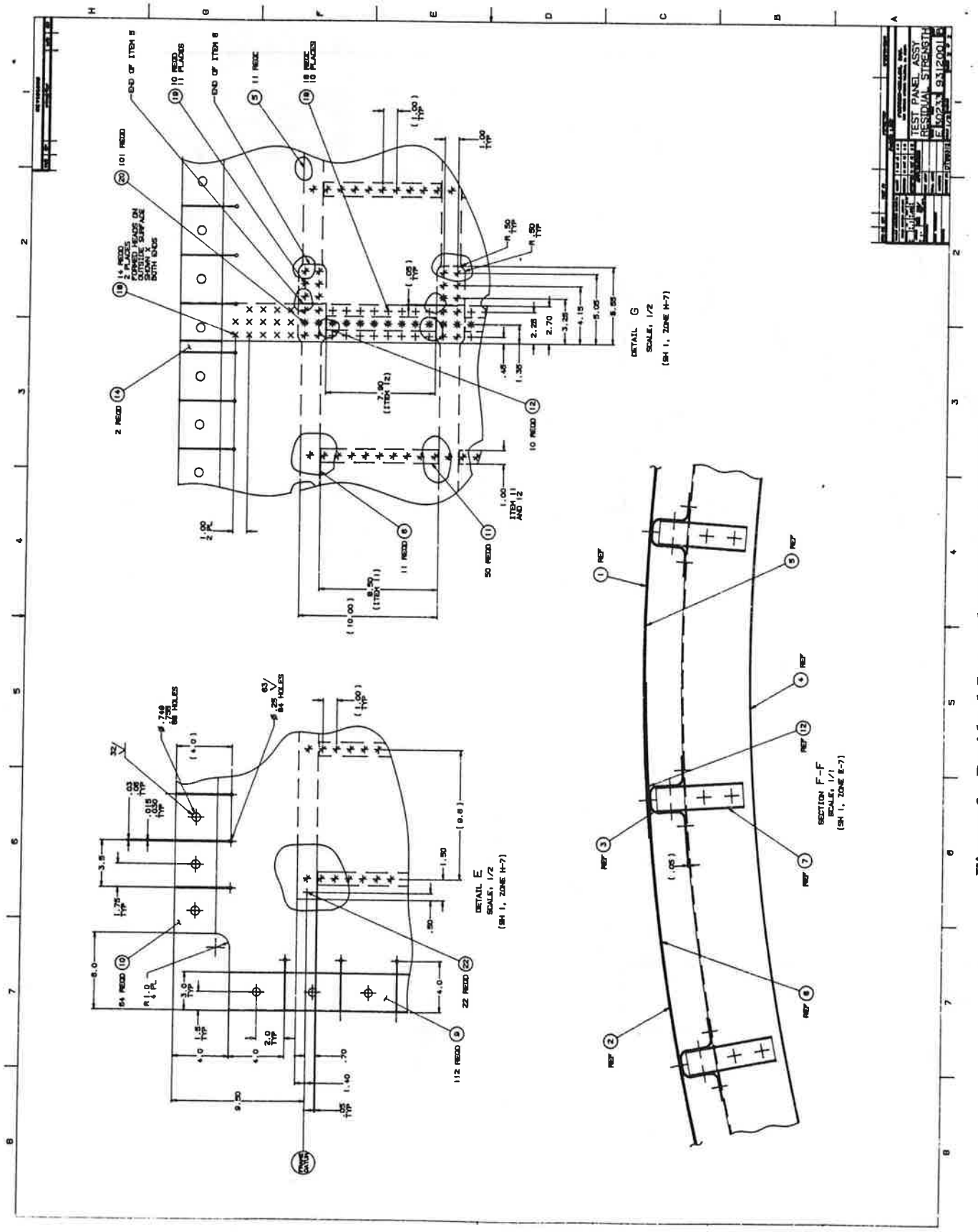

Figure 2. Residual Strength Test Panel Details

Table 2. Panel Features

Panel length (in.)	120
Panel width (developed) (in.)	68
Panel radius (in.)	75
Number of frames	6
Number of tear straps	11
Number of stringers	6
Frame spacing (in.)	20
Tear strap spacing (in.)	10
Stringer spacing (in.)	9.6
Skin thickness (in.)	0.04
Tear strap thickness (in.)	0.04
Skin and tear strap material	2024T3 Aluminum alloy (clad)

the inside surface. This provides a smooth sealing surface for the test fixture fluid pressure seal. This rivet reversal has no influence on testing or panel performance since it is well clear of the central panel test region.

3.2 Fatigue Strength Panel

The configuration of the fatigue strength panel (9312002) is shown in Figures 3 and 4. Major panel features are the same as for the residual strength panel and are listed in Table 2.

The only difference between the fatigue and residual strength panel configurations is the design of the longitudinal panel to fixture attachment. The 28 individual fingers are replaced by an unslotted arrangement and increased doubler thickness. Attachment hole diameters have also been increased from 0.75 in. to 1.00 in. diam. The skin is reinforced by six bonded 0.04 thick doubler sheets. This arrangement was developed during Panel 12 testing to prevent fatigue damage at the attachments.

An alternate fatigue strength panel configuration has been designed and two panels (Panels 13 and 17) have been built. Neither panel has been tested. The panel configuration (9312003) is shown in Figures 5 and 6. The panel is the same as the 9312002 configuration except that the lap joint orientation has been reversed. That is, the inner skin and outer skin were reversed. This change has been made to determine whether the asymmetric panel arrangement influences lap joint fatigue performance.

3.3 Manufacturing Considerations

Influences of a number of manufacturing variables on panel performance were studied during the program. This study was prompted by the lower rivet row skin failures which occurred under fatigue loading of Panel 7 in the previous test series (1) and the similar failure of Panel 12 in this test series. The variables that have been studied are:

- Lap joint and tear strap widths.
- Rivet bucktail diameters.
- Upper skin rivet hole knife edge.
- Lap joint location.

These issues are briefly described in the following subsections.

3.3.1 Lap Joint and Tear Strap Widths

Panel 7 (1) was built with a 3.34 in. wide lap joint and 1 in. wide tear straps. Fatigue failure occurred at the lower rivet row. This failure mode was unexpected and may have been caused by the abnormally high pressure range (1 to 13 psig) or by the lap joint geometry. Post-failure analysis of the panel by Dr. Pelloux (3) found that the lower skin failure was initiated at fretting cracks on the lower skin outer surface. Fatigue failure was due to tensile and bending loads on the lower skin at the lower rivet line.

All panels in this test series have a 2.7 in. wide lap joint and 1.4 in. wide tear straps. This con-

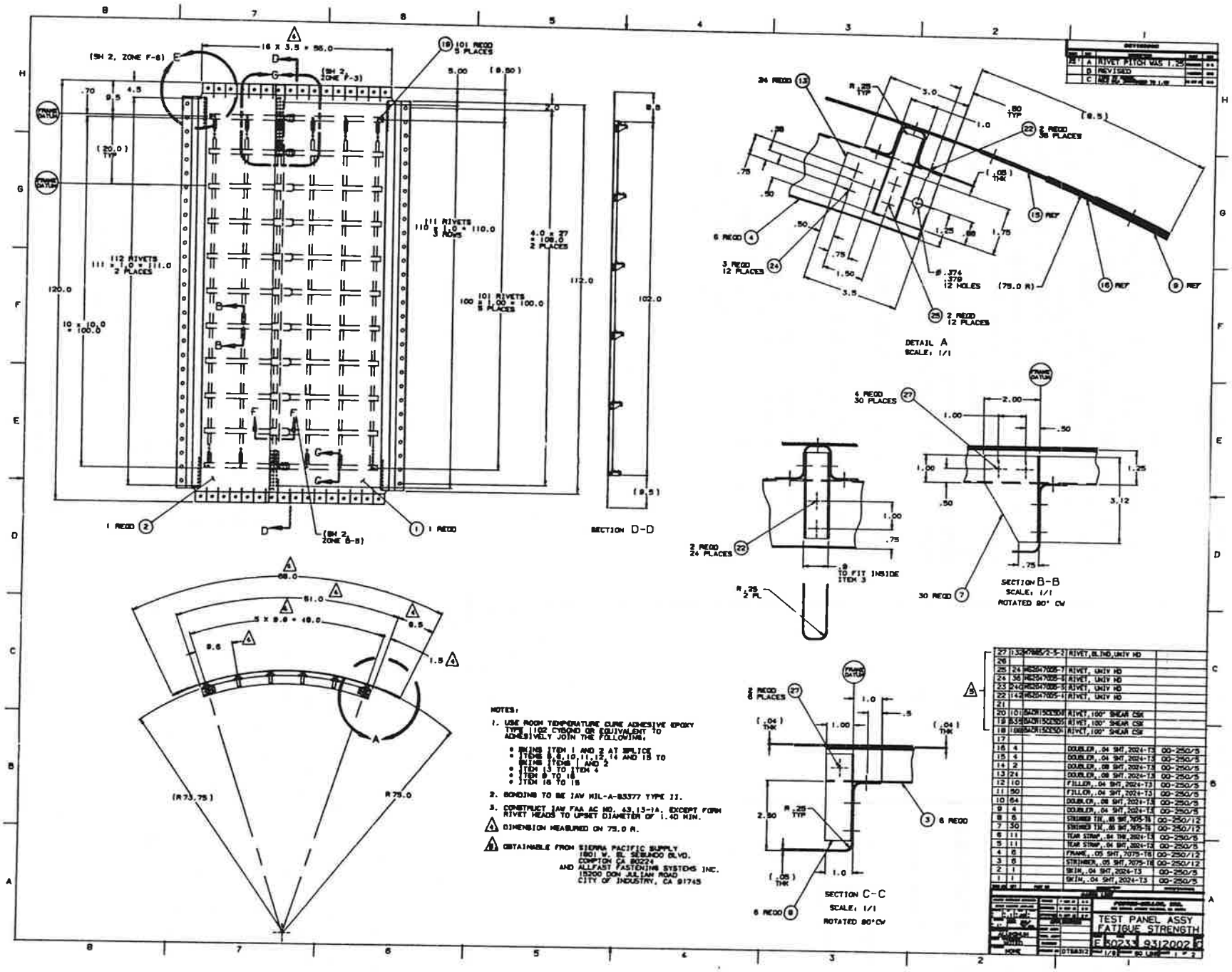

Figure 3. Fatigue Strength Test Panel

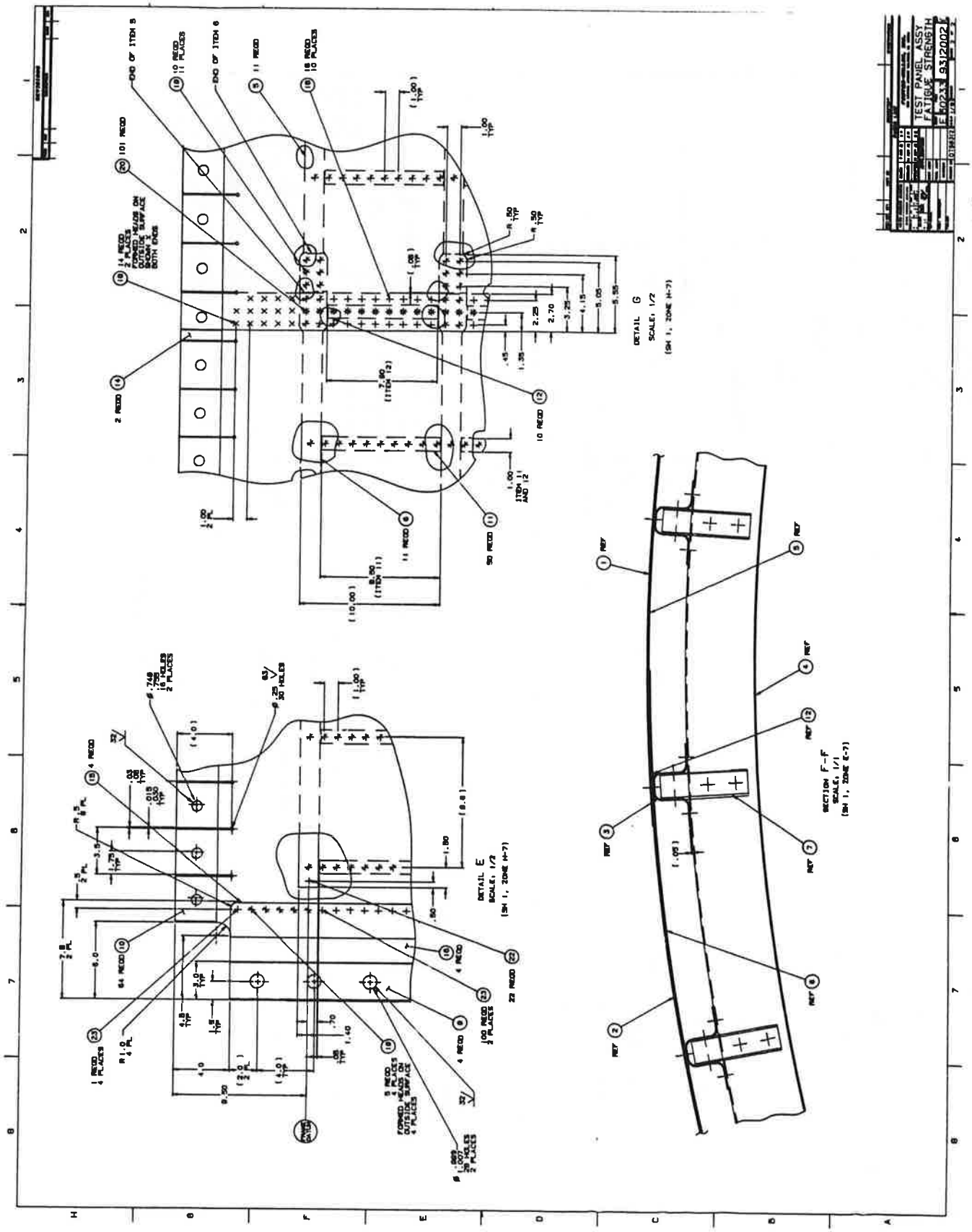

Figure 4. Fatigue Strength Test Panel Details

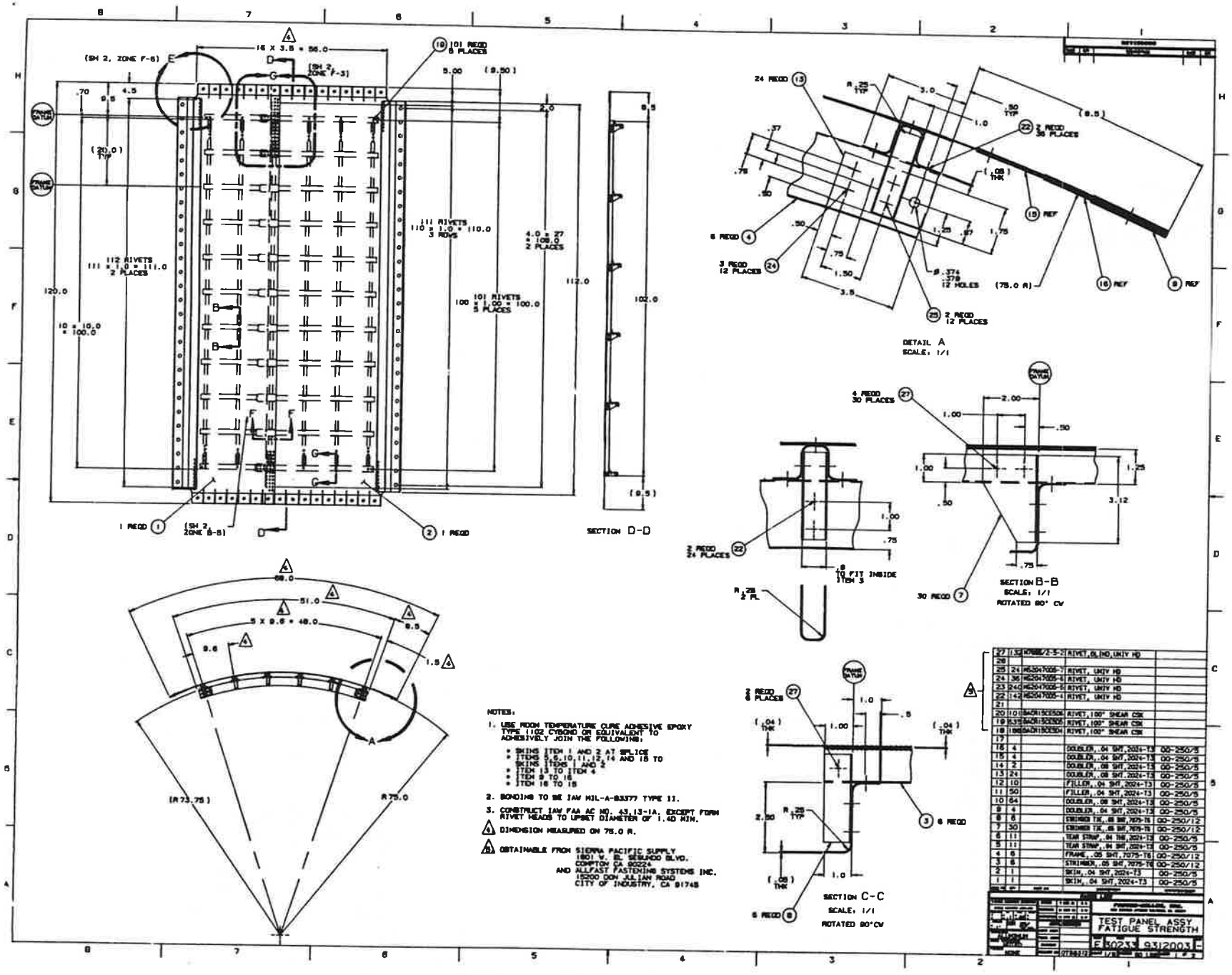

Figure 5. Alternate Fatigue Strength Test Panel

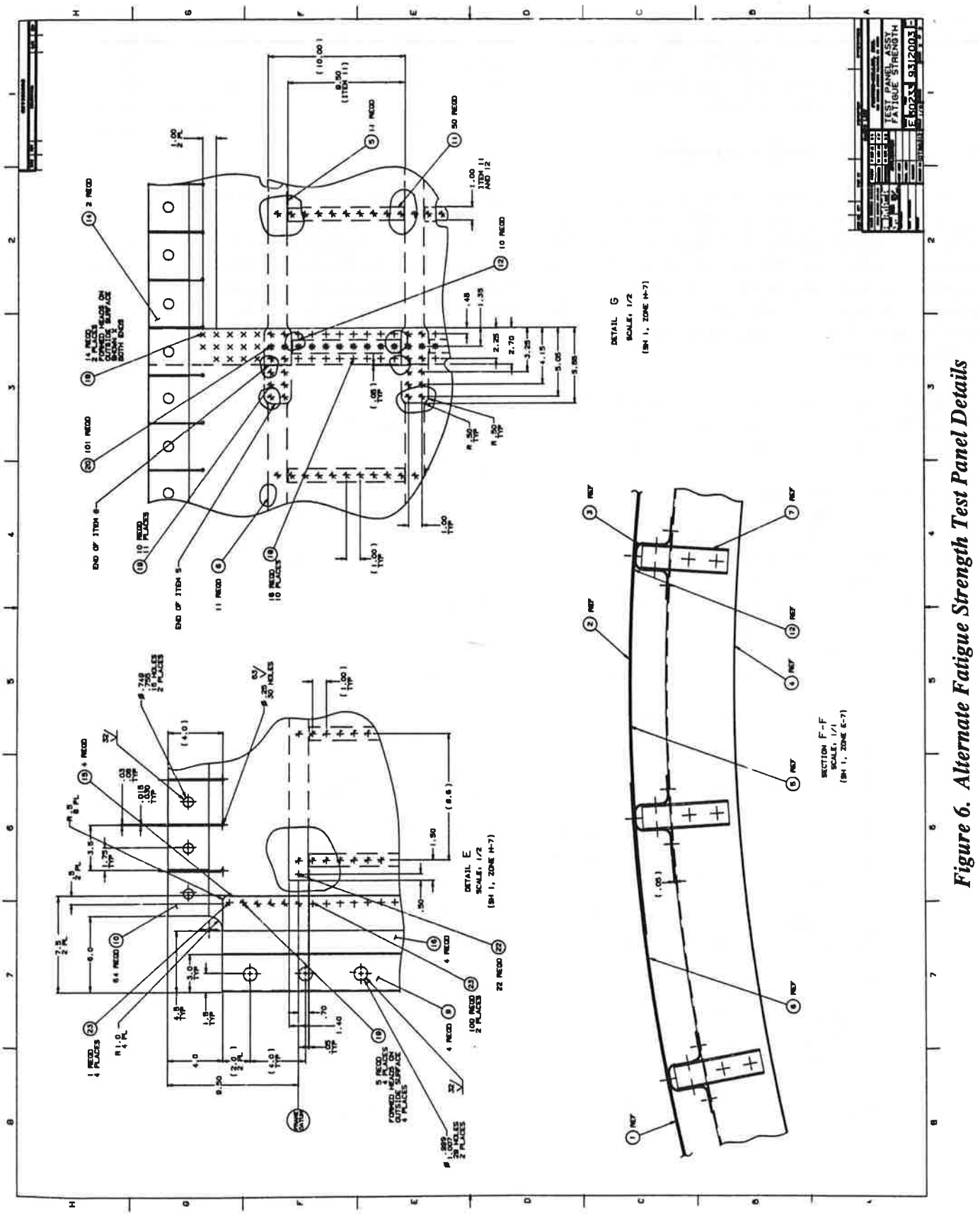

Figure 6. Alternate Fatigue Strength Test Panel Details

figuration is very similar to lap joints used on B707, B727 and B737 type aircraft. The wider tear strap provides a slight improvement in lower skin bending stiffness and a substantial increase in upper skin bending stiffness.

3.3.2 Rivet Bucktail Diameters

Panel 7 lap joint rivets were installed in accordance with FAA AC NO. 43.13-1A (4) which requires rivet bucktail diameters of 1.5d minimum where d is the rivet diameter. Boeing experience according to Dr. Gorenson (5) is that lower row lap joint damage can occur with overbucked rivets. Boeing uses rivets bucked to 1.4d minimum.

Bucktail diameters for all panels manufactured during this test series (Panels 8 through 17) were manufactured to the 1.4d specification.

Actual bucktail diameters were measured on Panel 7 and Panel 12. Diameters were also measured on aircraft panel specimens from a B707 and a DC10 provided by VNTSC and on a United Airlines B737-400 inspected by Foster-Miller personnel at Logan Airport in November 1991. The results of this measurement survey are summarized in Table 3. The summary shows a significant change in bucktail diameters from Panel 7 to 12. Panel 12 is more consistent with industry practice than Panel 7. The B737 rivets show a high degree of consistency. These rivets are not lap joint rivets and are probably machine driven. Lap joint rivets show more variability because they are manually installed.

3.3.3 Upper Skin Rivet Hole Knife-Edge

Cracking at lap joint upper rivet row joints is believed to start at the stress concentration caused by the knife-edge in the upper skin formed at the base of the countersunk rivet head. The sharper this knife-edge the greater the stress concentration. Manufacturing variables affecting sharpness include:

- Skin thickness.
- Rivet head height.
- Rivet head protrusion.
- Countersink hole depth.
- Rivet squeeze.

The effects of these variables are briefly described below.

Table 3. Bucktail Rivet Diameter Summary

Assembly	No. Rivets	Rivet Diameter (in.)	Rivet Bucktail Diameter (in.)		
			Minimum	Maximum	Range
Foster-Miller Fatigue Panel 7 Lap	90	5/32	1.47	1.77	0.30
Foster-Miller Fatigue Panel 12 Lap	95	5/32	1.26	1.48	0.22
B707 Lap	25	3/16	1.38	1.60	0.22
DC10 Lap	112	3/16	1.27	1.54	0.27
B737 Stringer	75	5/32	1.37	1.46	0.09

Panel skin thickness used for all test panels manufactured to date is 0.040 in. The B737 skin thickness is 0.036 in. The thicker skin has been used for the test panels because it is a standard gauge and is readily available at reasonable cost. Use of the thicker skin effectively reduces the knife-edge sharpness by 0.004 in.

The 5/32 in. diam shear head 100 deg countersink rivets used, Part No. BACR15CE5D, have a maximum specified head height of 0.039 in. Sample measurements were made of the head heights of 84 rivets of the three different lengths used for panel manufacture using an optical microscope. Head heights ranged from 0.030 in. minimum to 0.044 in. maximum. Average head height was 0.038 in.

The test panels have been manufactured to satisfy Boeing aerodynamic flushness requirements. Allowable head protrusions are 0 to +0.004 in. for 90 percent and ±0.005 for 10 percent. Measured upper rivet row rivet head protrusions on Panel 12 ranged from 0.002 to 0.007 in. Average head height was 0.005 in. Panel rivet protrusions using the fingernail test appeared similar to the B737-400 fuselage lap joints examined.

The countersink hole depth is drilled to the depth required to achieve a satisfactorily installed rivet. Examination of this depth during manufacture showed the depth to be approximately 0.028 in. leaving a 0.012 in. blunt knife-edge. Subsequent rivet installation resulted in 0.002 to 0.007 in. protrusions. When hole depth was increased to achieve a knife-edge the installed rivet became recessed between 0.001 and 0.003 in. An intermediate countersunk hole depth with a 0.007 in. blunt knife-edge provided satisfactory 0 to +0.002 in. protrusions. This approach was taken in building Panel 16. When tested Panel 16 showed some leakage at the rivets. Leakage was not present on previous panels.

Measurements taken of countersink hole depth and rivet head heights before and after installation shows a change in rivet squeeze characteristics as the depth of the countersunk hole is increased. The greater the initial head protrusion the greater the head volume that is "lost" in hole filling. This results in a tighter joint and can cause some skin deformation.

While the results of this manufacturing study are somewhat anecdotal certain trends do appear. The results are summarized in Table 4. The four variables discussed are listed and probable combinations are shown. Using average uninstalled rivet head heights and protrusions for the B737 an estimate of the knife-edge bluntness and rivet head shrinkage can be made. The same rationale can be used for panels fabricated to date. Efforts should be made to ensure that future panels limit the uncountersunk depth of lap joint upper row rivets to 0.007 in. All remaining rivets should maintain the 0.012 in. depth to prevent unnecessary leakage. This approach has been taken in the fabrication of untested Panels 13 and 17.

3.3.4 Lap Joint Location

The test fixture design is such that the pressurized panel experiences a small non-representative bending load. This bending load occurs because the panel longitudinal edges are restrained and the panel is only free to deflect at its center. Both deflection and strain measurements across the lap joint region indicate significant bending of the lower skin away from the lap joint. Under fatigue loading this bending results in eventual panel failure at the lap joint lower rivet row. The panel section bending stiffness is considerably lower at the lap joint bottom skin than it is at the top because of the lap orientation and the additional thickness provided at the top by the tear strap lap joint. In addition, the lower skin is closer to the anchored panel edge possibly further contributing to the non-representative bending that occurs. While the lap joint configuration being representative should not change, the lap joint location on the panel can be changed by changing the widths of the upper and lower skins to position the lap joint at a different stringer. Such a change has been incorpo-rated in Panels 13 and 17. In these panels the lap joint has been reversed to make the lower skin furthest from the anchored panel edge.

Table 4. Rivet Installation Characteristics

Feature		B737		Test Panel			
		Apparent	Probable Typical	Probable Typical	Probable Range		Panel 16
Uninstalled rivet head height (in.)	H	0.039	0.038	0.038	0.030	0.044	0.038
Uncountersunk depth (in.)	B	0.000	0.007	0.012	0.012	0.012	0.007
Rivet head shrinkage (in.)	S	0.000	0.007	0.010	0.002	0.009	0.003
Rivet head installed protrusion (in.)	P	0.003	0.002	0.005	0.000	0.007	0.002
Skin thickness (in.)	T	0.036	0.036	0.040	0.040	0.040	0.040

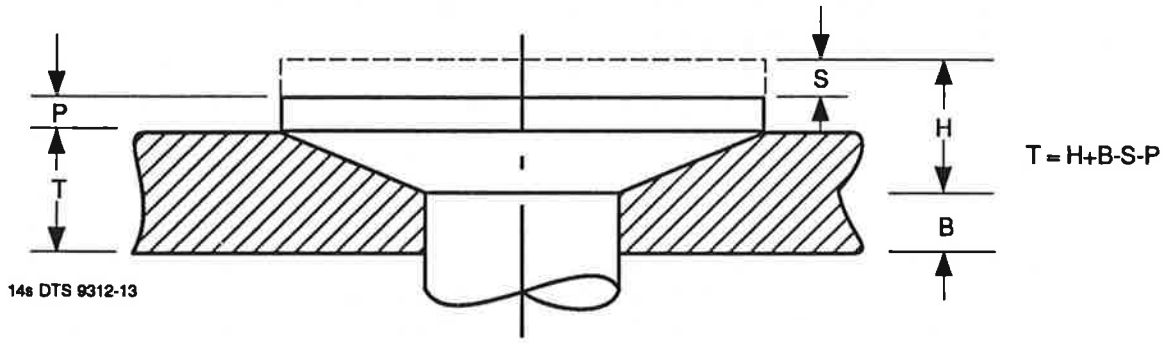

4. PANEL RESIDUAL STRENGTH TESTS

A total of seven panel residual strength tests were performed as summarized by Table 5. The purpose of these tests was to evaluate the residual strength of panels with long lead cracks in the upper rivet row of the lap splice. Further, the effect of MSD beyond the lead crack tips was investigated. The direction of crack propagation (flapping or non-flapping) was an important result. One test (Panel 16) was conducted to investigate the effect of a broken frame on the panel residual strength.

Test data and correlations with analytic predictions follow. The residual strength is expressed in terms of panel internal pressure at the onset of fast crack growth. Hoop and longitudinal stresses were measured with strain gauges. Crack propagations in the first ligaments beyond the lead crack tips were measured with an indirect DC potential drop system. The relationships between crack propagation and applied pressure are shown in Figure 7. The following subsections discuss the results of each test.

4.1 Panel Nos. 8, 9 and 16 (24 in. Lead Crack)

Panel Nos. 8, 9 and 16 were fabricated with a 23.36 in. lead crack in the upper rivet row of the lap splice. All three panels had completely unbonded lap splices. Panel No. 9 also contained MSD on five rivet holes beyond the lead crack tips. The tip-to-tip MSD crack lengths were 0.36 in. inclusive of the rivet hole. Panel No. 16 contained the same MSD as Panel No. 9 and a broken frame (F3) at stringer S3.

The outer surface of the panels was instrumented as shown in Figure 8. A total of 11 strain gauges were applied with an additional six gauges applied to the inner surface of Panel No. 8 as indicated by the circles. Crack propagation gauges were applied at the lead crack tips to record growth in the first ligaments. Applied panel pressure and loading system hydraulic pressure were measured with pressure transducers. The applied load of the test machine was also output to the data acquisition system. Videotape provided an additional record of the tests.

Static tests were performed on each panel to record strain-pressure relationships at all gauged locations. The measurements from Panel No. 16 were comparable to Panel Nos. 8 and 9. Based on this data, five strain gauges were selected (see Figure 8) to be recorded during loading to failure. This reduction was made to permit a faster data sampling rate. These five strain gauges, the two crack propagation gauges, and the applied panel pressure were recorded at a rate of four samples/ sec during failure loading.

For the failure tests of Panels 8 and 9, the internal panel pressure was increased at a constant rate of 1 psi per second. Stable crack growth began in Panel No. 8 at approximately 7 psi. The total crack extension reached 0.1 in. at 8.6 psi. The center tear strap at F3 failed at 9.4 psi. From review of the videotape, (referring to the F3 tear strap failure as time zero) the tear strap between F2 and F3 failed at 0.37 sec and the tear strap between F3 and F4 failed at 0.40 sec. The tear strap at F2 then failed at 0.70 sec and pressurization could not be maintained. The final crack is shown in Figure 9. A photograph of the failed panel is shown in Figure 10.

Stable crack growth began in Panel No. 9 at approximately 6.2 psi. The total crack extension reached 0.1 in. at 7.5 psi. The center tear strap at F3 and the midframe bay tear straps on either side of F3 all failed at 10.5 psi. From the crack

Table 5. Summary of Residual Strength Tests on Panels with MSD in Lap Splices

CASE NO.	FM PANEL NO.	LEAD CRACK LENGTH (in.)	NO. OF RIVETS WITH MSD (EACH SIDE OF LEAD CRACK)	FAILURE PRESSURE (psi)	DID FLAPPING OCCUR?	WAS CRACK ARRESTED AT **NEXT** TEAR STRAP OR FRAME?	DISTANCE FROM LEAD CRACK OR MSD CRACK TIP TO CENTER OF NEXT TEAR STRAP (in.)	CONFIGURATION DOUBLE LINE: LEAD CRACK SINGLE LINE: FINAL FRACTURE (MSD AT RIVETS NOT SHOWN) F_1 F_2 F_3 F_4 F_5 F_6
1	8	23.36	NONE	8.6	NO	NO	8	
2	9	23.36	5	7.5	YES	YES	3	
3	10	29.36	NONE	6.9	NO	YES	5	
4	11	29.36	5	6.1	NO	NO	10	
5	14	35.36	NONE	6.1	YES	YES	2	
6	15	35.36	5	5.9	NO	NO	7	
7	16	23.36*	5	NR	NO	YES	3	

14s DTS 9312-14s

NR - NOT RECORDED
* - BROKEN FRAME

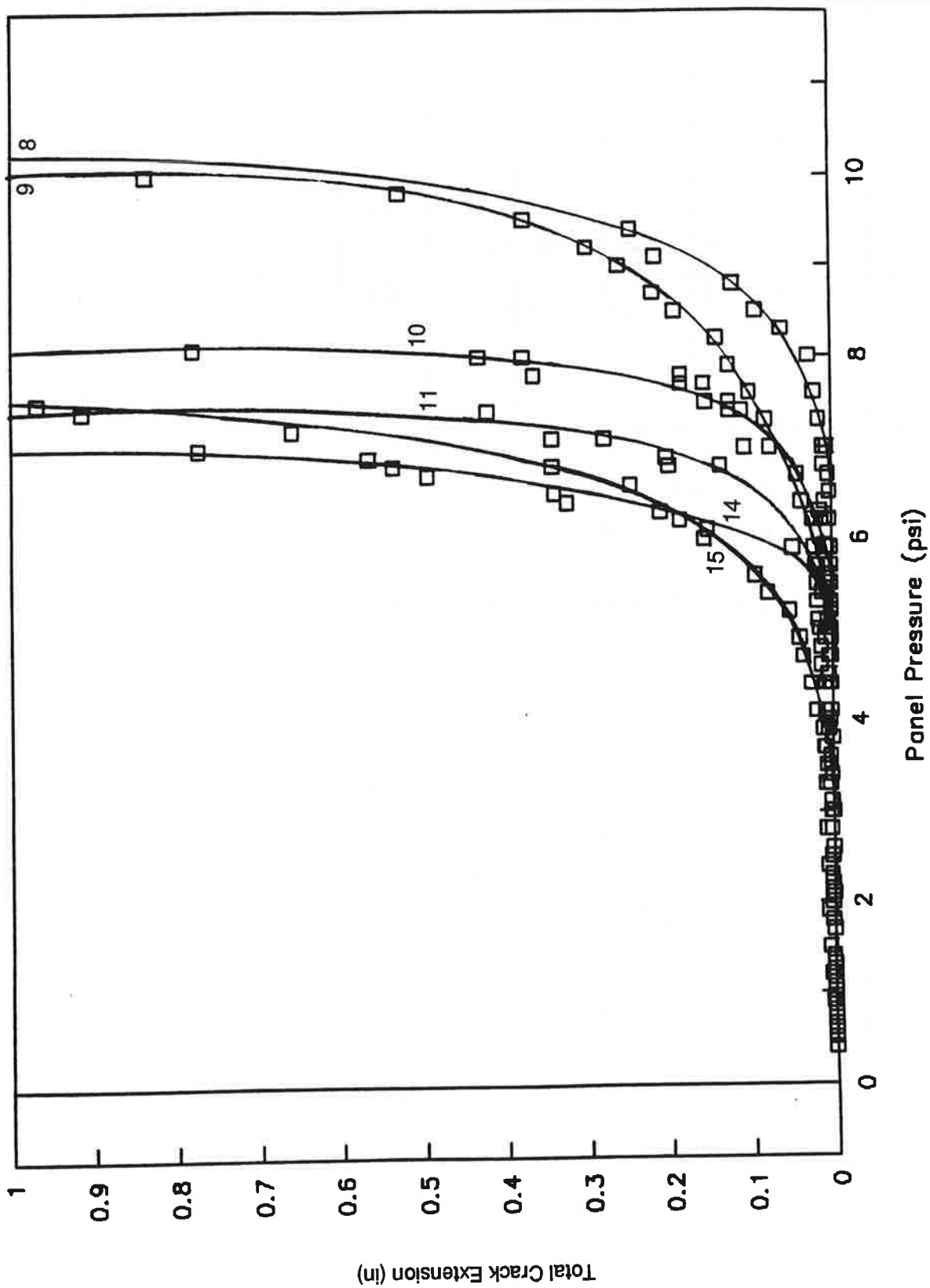

Figure 7. Crack Propagation in Residual Strength Tests

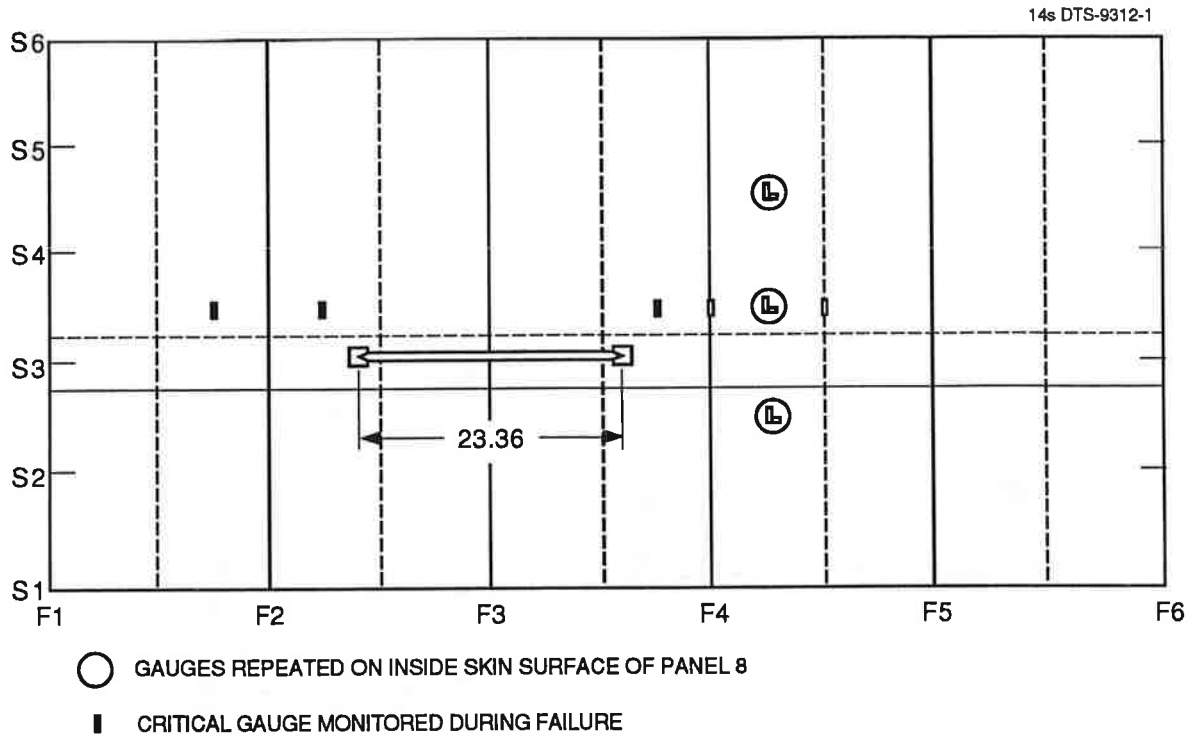

Figure 8. Panel Instrumentation (Panel 8 shown)

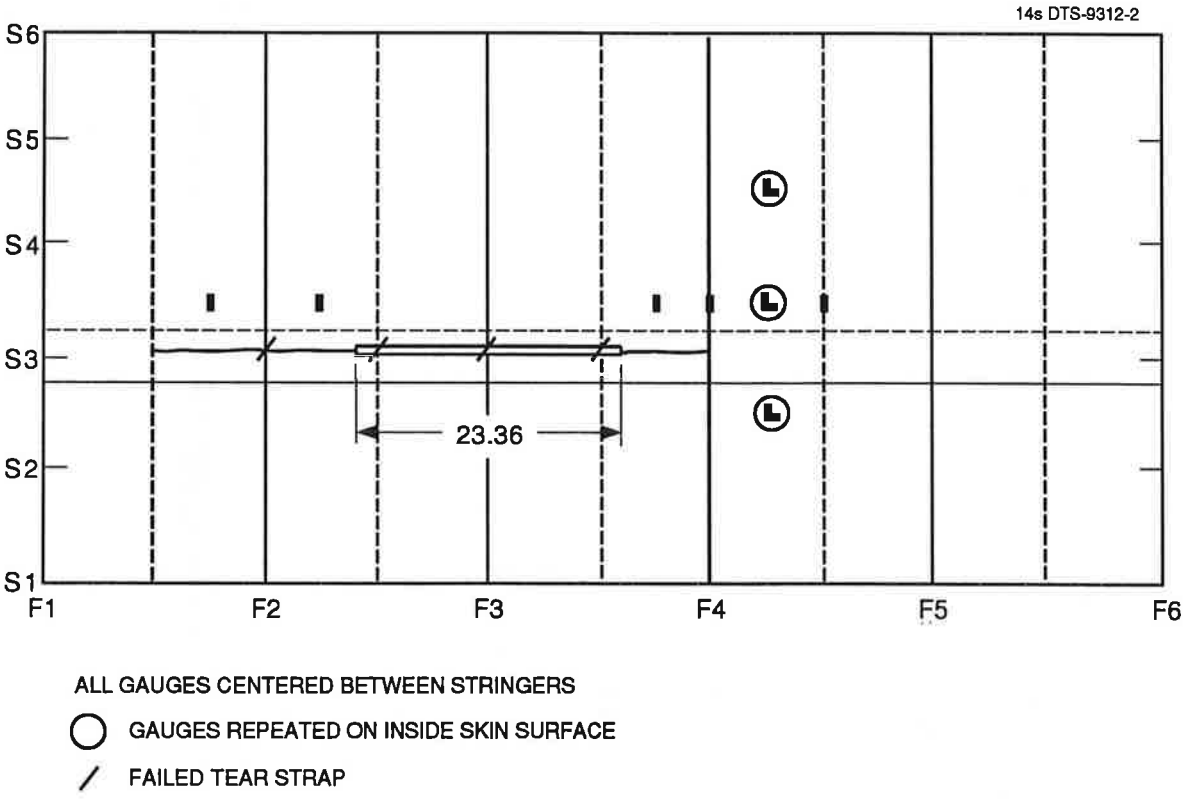

Figure 9. Panel 8 - After Fracture

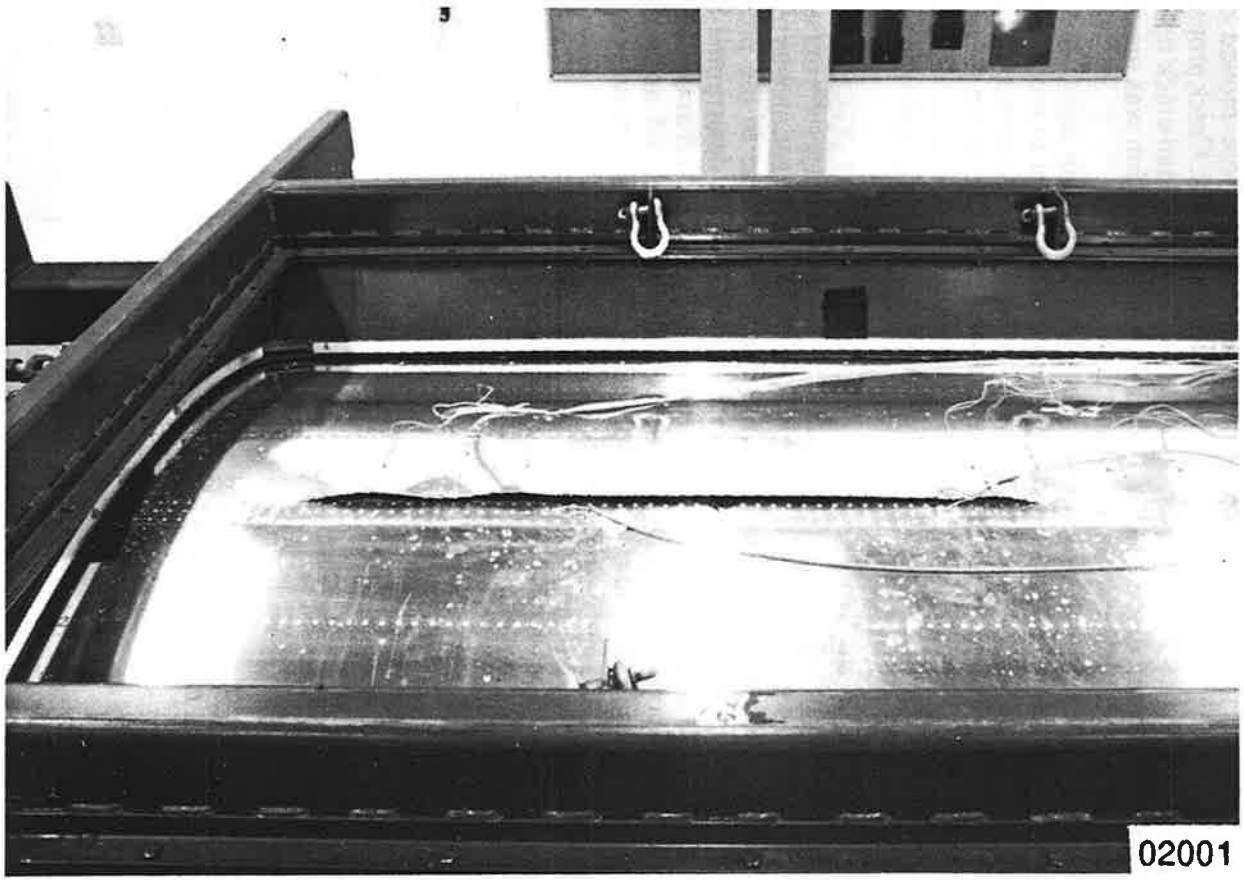

Figure 10. Panel 8: 23.36 in. Crack, No MSD - After Fracture

propagation gauges and the close-up videotape, it is evident that the first ligaments past the lead crack tips failed completely approximately 2 sec prior to the tear strap failures. Further from the videotape, the crack turns at F2, resulting in a flapping failure, 0.27 sec after failure of the tear straps. The final crack is shown in Figure 11. A photograph of the failed panel is shown in Figure 12.

For the failure test of Panel No. 16, the incremental loading procedure, discussed in subsection 5.2, was used. Due to "Krak Gage" bonding problems, stable crack growth was not recorded. Failure of the three center tear straps occurred at 9.6 psi. The crack grew in both directions to the next frame. The final crack is shown in Figure 13a. A photograph of the failed panel is shown in Figure 13b.

4.2 Panel Nos. 10 and 11 (30 in. Lead Crack)

Panel Nos. 10 and 11 were fabricated with a 29.36 in. lead crack in the upper rivet row of the lap splice. Both panels had completely unbonded lap splices. Panel No. 11 also contained MSD on five rivet holes beyond the lead crack tips. The tip-to-tip MSD crack lengths were 0.36 in. inclusive of the rivet hole.

The outer surface of both panels was instrumented with a total of 11 strain gauges. Gauge locations were the same as for Panel Nos. 8 and 9 to permit direct comparison. The exceptions were the two gauges nearest the crack tips which were moved slightly to be beyond the lead crack. Crack propagation gauges were applied at the lead crack tips and the other facility instrumentation was maintained.

As with the previous tests, static loading was applied to each panel to record strain-pressure relationships at all locations. Based on similar results, the same five strain gauges recorded in the tests of Panel Nos. 8 and 9 were selected for higher speed sampling during loading to failure.

The failure loading procedure was changed after review of the test results of Panel Nos. 8 and 9 Stable crack propagation was recorded by the instrumentation. Due to the pressure loading rate, it could not be determined if this growth would have proceeded at a constant pressure. As sealing of the panel did not present a major problem, all further testing was conducted under

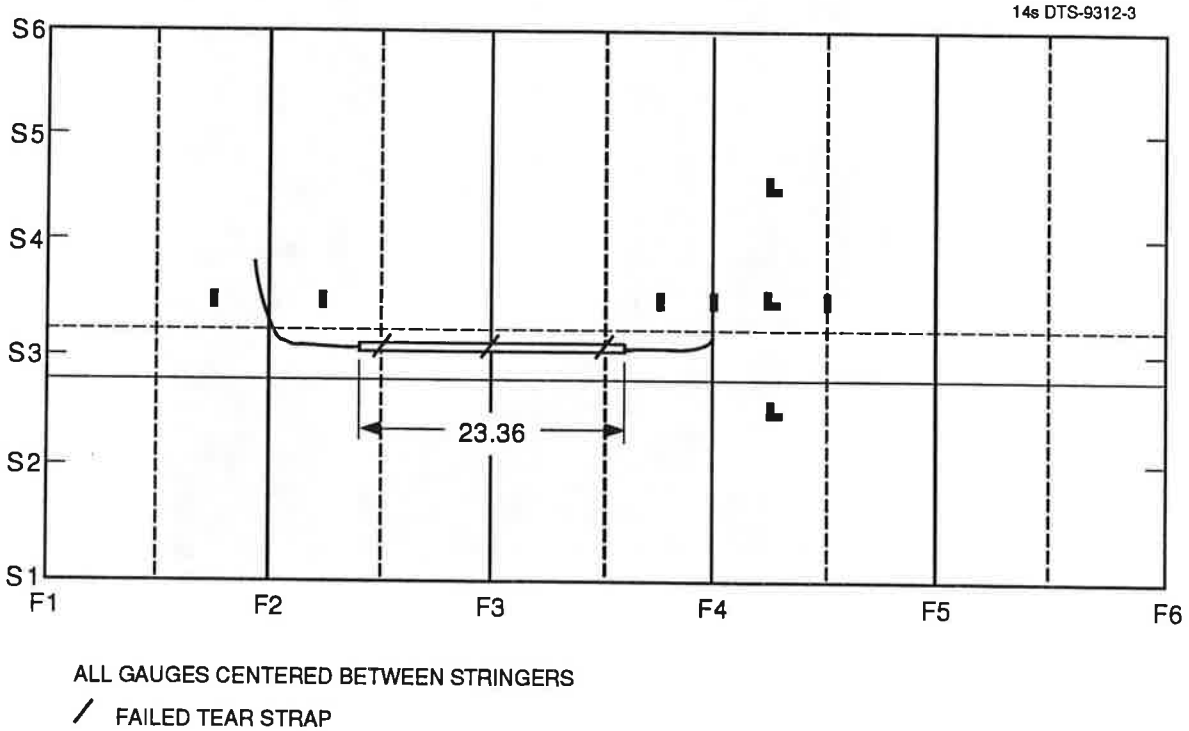

Figure 11. Panel 9 - After Fracture

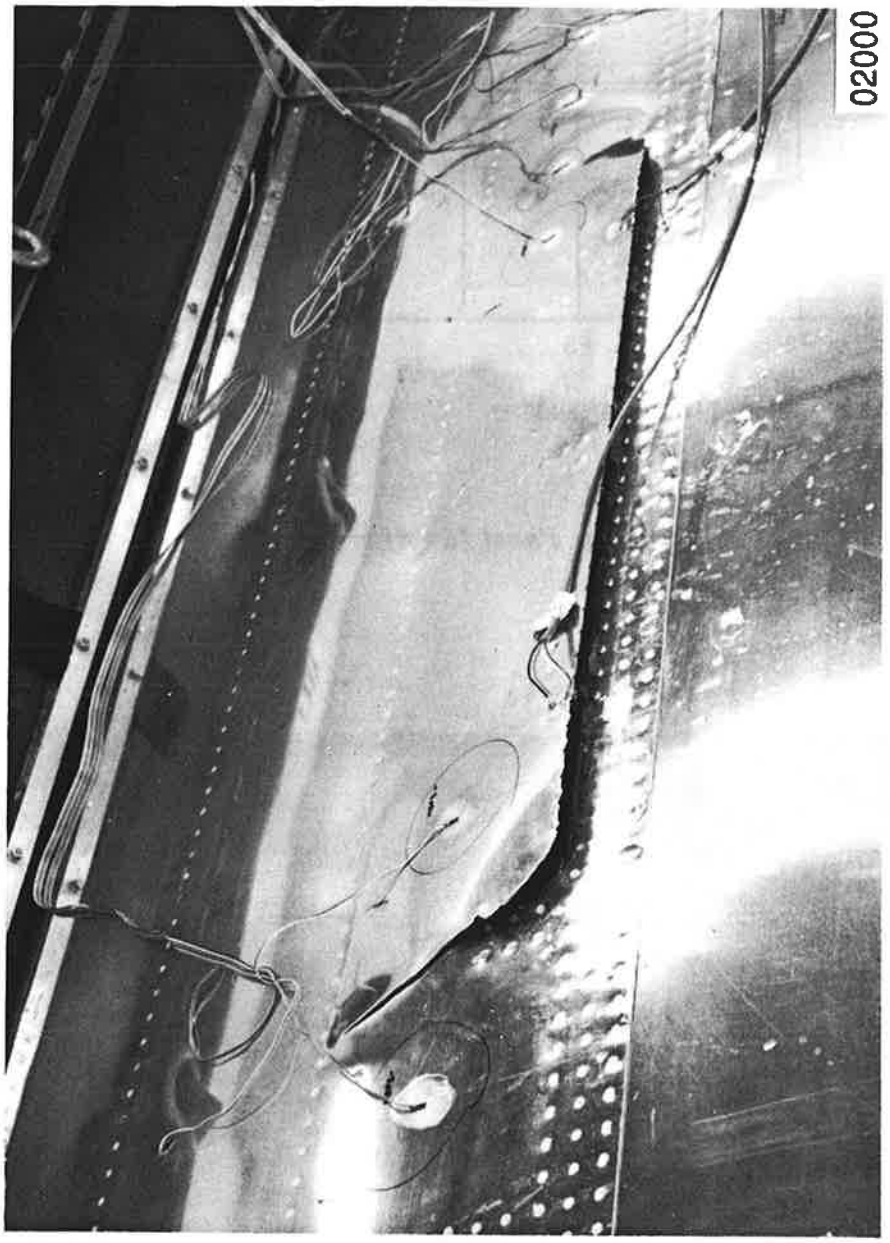

Figure 12. Panel 9: 23.36 in. Crack, MSD - After Fracture

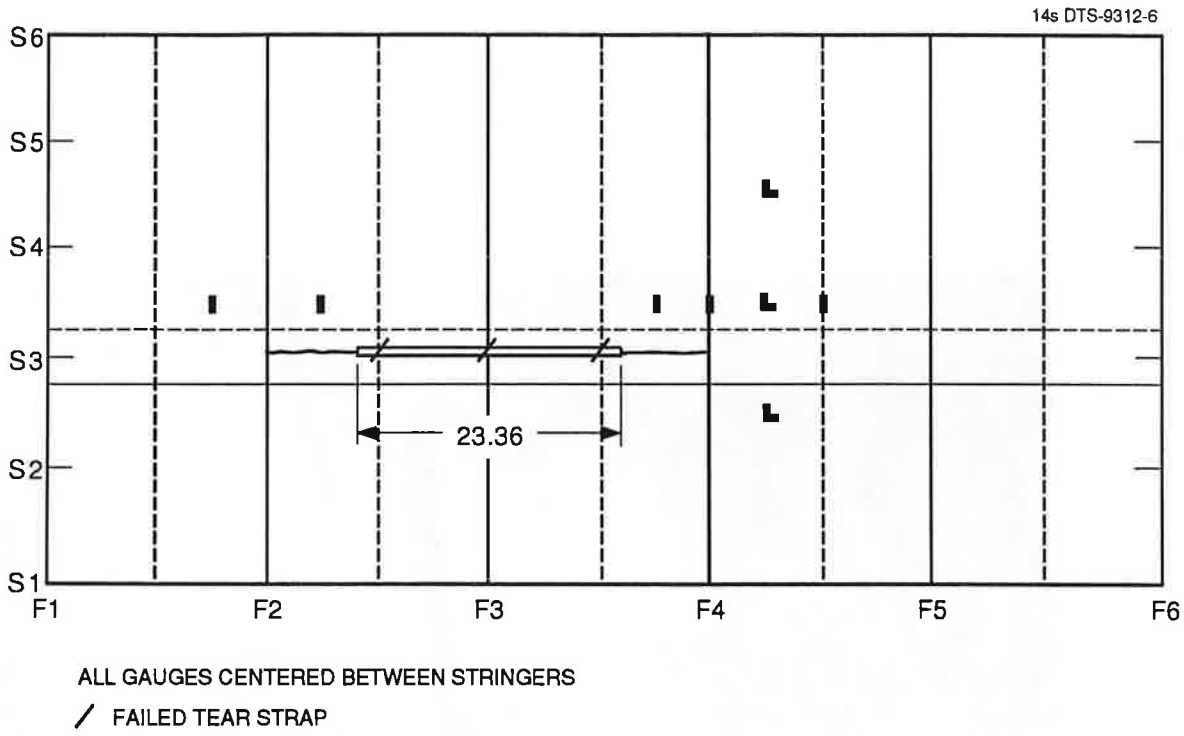

Figure 13a. Panel 16 - After Fracture

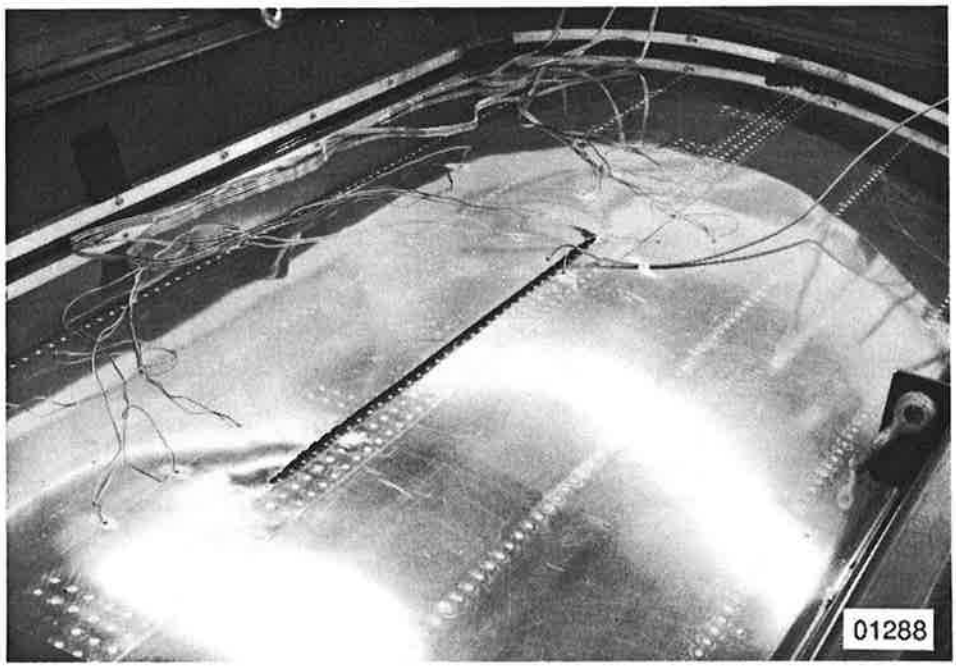

Figure 13b. Panel 16 After Fracture: 23.36 in. Crack, Broken Frame at F3

incremental pressure loading with static dwells when crack growth was recorded.

Stable crack growth was observed in Panel No. 10 at approximately 6.2 psi. The total crack extension reached 0.1 in. at 6.9 psi. The three center tear straps failed at 8.1 psi. From the crack propagation gauges, it is evident that complete failure of the first ligaments also occurred at 8.1 psi. The crack propagated in both directions to the next frame. The final crack is shown in Figure 14. A photograph of the failed panel is shown in Figure 15.

Stable crack growth began in Panel No. 11 at approximately 5.9 psi. The total crack extension reached 0.1 in. at 6.1 psi. While the pressure was held at 6.1 psi, stable crack growth continued and resulted in the complete failure of the first ligament on the lead crack tip nearer F4. Further incremental pressure increases were applied and failure of the first ligament nearer F2 was recorded at 7.4 psi. Failure of the three center tear straps occurred at 8.7 psi. The crack grew in both directions to the next frame. From review of the videotape, crack propagation stopped for 0.7 sec and then the tear strap at F2 failed and the crack grew to the tear strap between F1 and F2. The final crack is shown in Figure 16. A photograph of the failed panel is shown in Figure 17.

4.3 Panel Nos. 14 and 15 (36 in. Lead Crack)

Panel Nos. 14 and 15 were fabricated with a 35.36 in. lead crack in the upper rivet row of the lap splice. Both panels had completely unbonded lap splices. Panel No. 15 also contained MSD on five rivet holes beyond the lead crack tips. The tip-to-tip MSD crack lengths were 0.36 in. inclusive of the rivet hole.

The outer surface of both panels was instrumented with a total of 10 strain gauges. Gauge locations were mostly the same as those of the previous panels to permit direct comparison. The exceptions were the gauge nearest the F4 lead crack tip which was eliminated and the gauge nearest the F2 lead crack tip which was moved to directly over the tear strap between F1 and F2. Crack propagation gauges were applied at the lead crack tips and the other facility instrumentation was maintained.

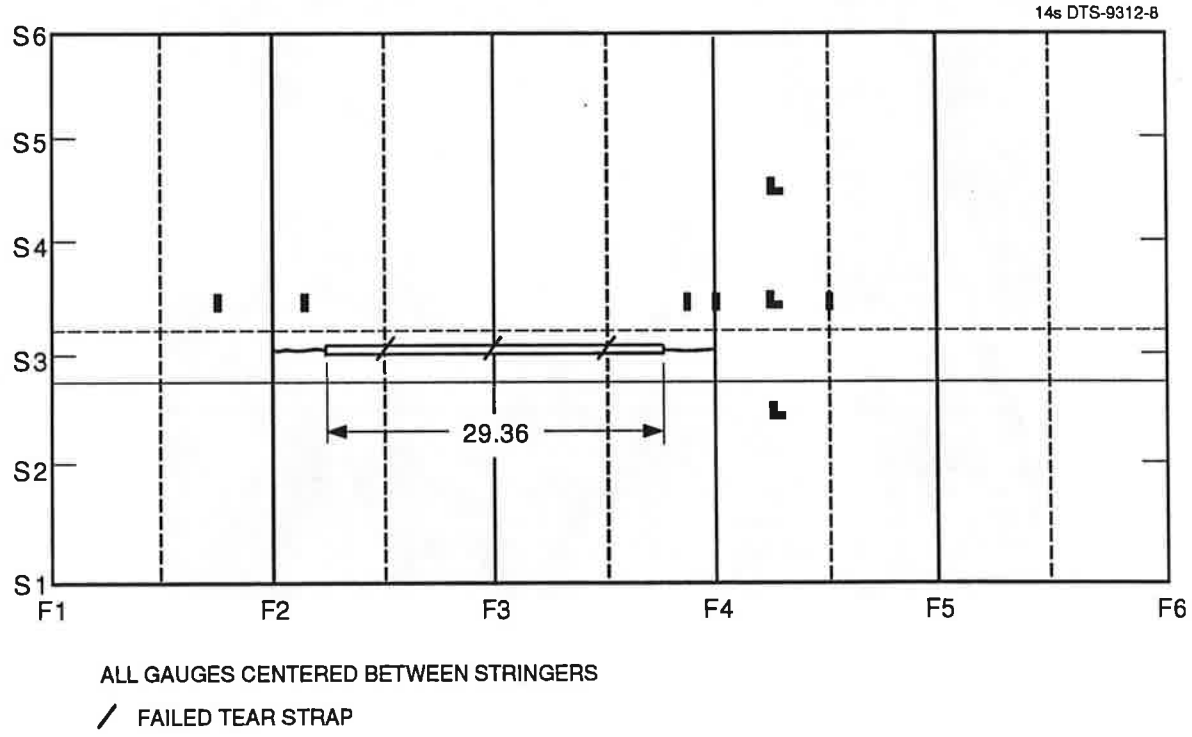

Figure 14. Panel 10 - After Fracture

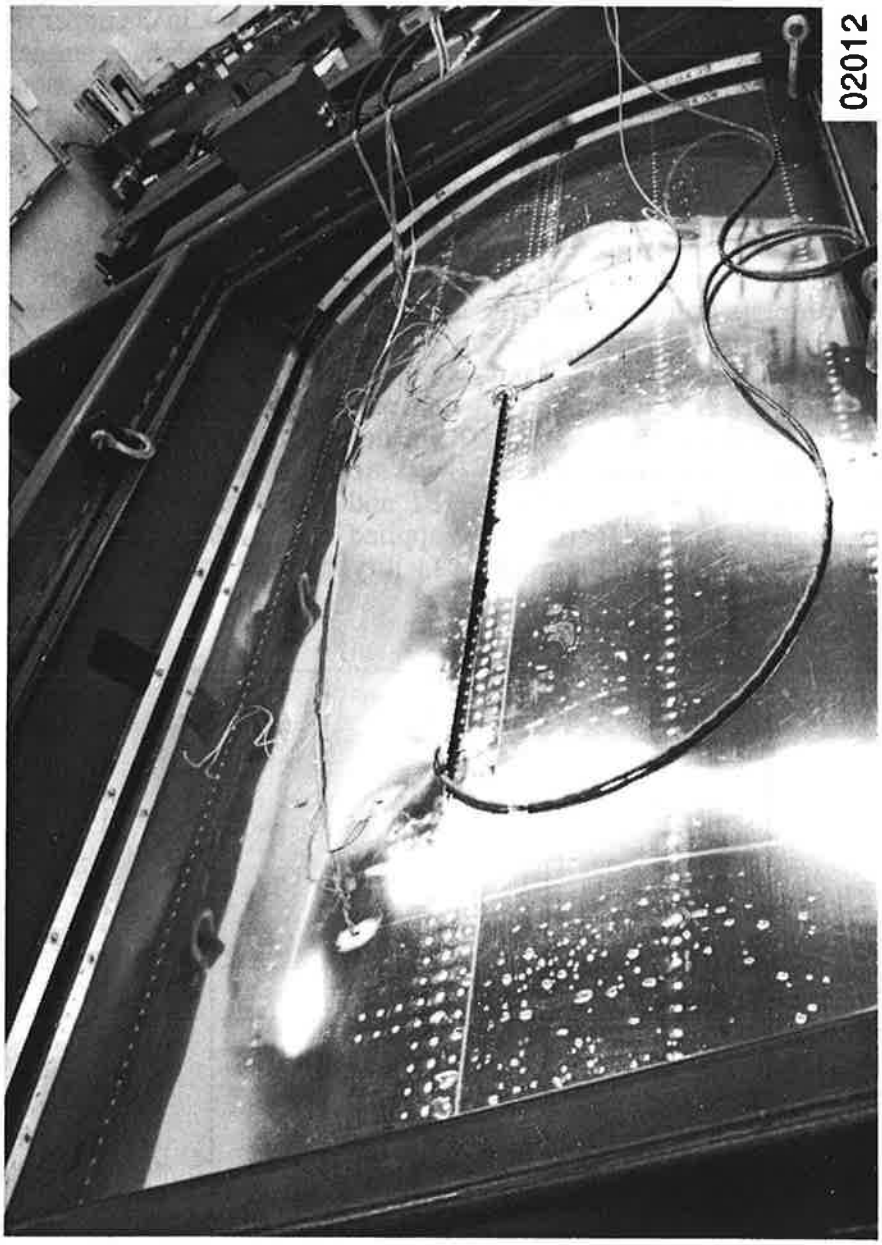

Figure 15. Panel 10: 29.36 in. Crack, No MSD - After Fracture

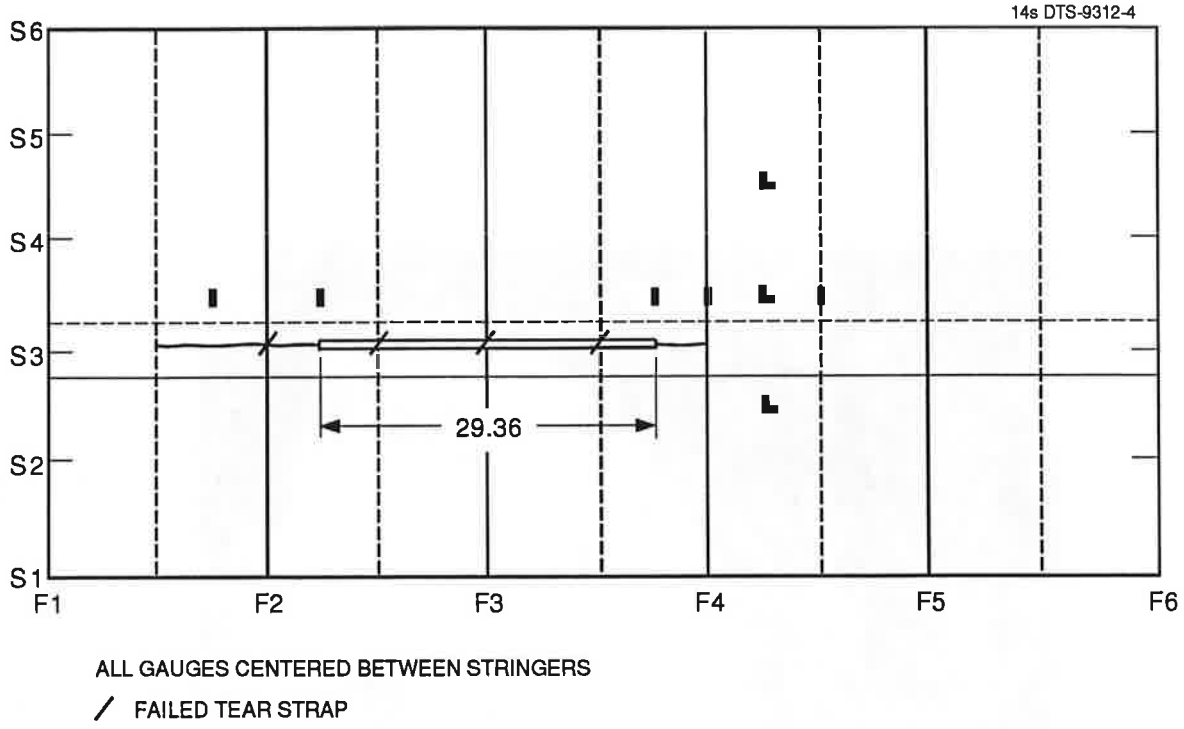

Figure 16. Panel 11 - After Fracture

As with the previous tests, static loading was applied to each panel to record strain-pressure relationships at all locations. Based on similar results, the four of the five strain gauges recorded in the previous tests were selected for higher speed sampling during loading to failure. As one gauge had been eliminated, an alternative fifth gauge was selected based on the potential crack growth path.

The incremental pressure loading procedure used in the failure tests of Panel Nos. 10 and 11 was followed. Stable crack propagation was recorded at constant pressure and thus incremental loading was considered to be a more correct failure test procedure.

Stable crack growth was observed in Panel No. 14 at approximately 5.1 psi. The total crack extension reached 0.1 in. at 6.1 psi. Stable crack growth resulted in the failure of the first ligament nearer F4 at 7.1 psi. A further incremental pressure increase was applied and failure of the first ligament nearer F2 was recorded at 7.3 psi. Failure of the three center tear straps occurred at 7.4 psi. The crack grew in both directions to the next frame and then turned approximately 1 in. away from the lap splice. From review of the videotape, the turned crack at F2 continued to grow after 1.1 sec and progressed to 7.5 in. away form the lap splice. The tear strap at F2 did not fail. The final crack is shown in Figure 18. A photograph of the failed panel is shown in Figure 19.

Stable crack growth was observed in Panel No. 15 at approximately 3.5 psi. The total crack extension reached 0.1 in. at 5.9 psi. Stable crack growth resulted in the failure of the first ligament nearer F4 at 7.2 psi. Further incremental pressure increases were applied and failure of the first ligament nearer F2 was recorded at 7.8 psi. The center three tear straps also failed at this time and the crack grew in both directions to the next frame. The tear strap at F2 failed 0.7 sec later and that crack tip began to grow toward the next tear strap. At 0.9 sec after initial failure, the crack had propagated to the tear strap between F4 and F5. At this same time, the tear strap at F2 failed, the crack grew immediately to the next tear strap, and pressure could not be maintained. The final crack is shown in Figure 20. A photograph of the failed panel is shown in Figure 21.

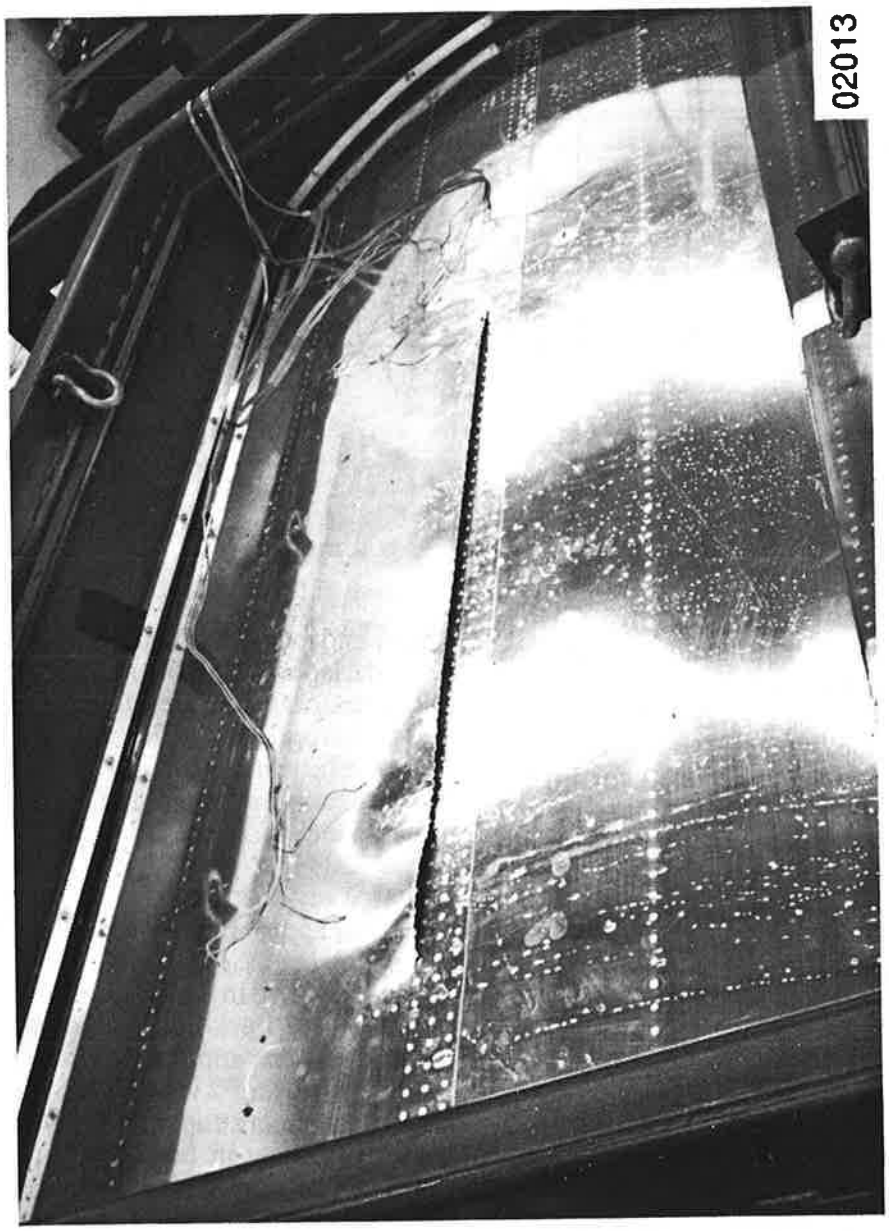

Figure 17. Panel 11: 29.36 in. Crack, MSD - After Fracture

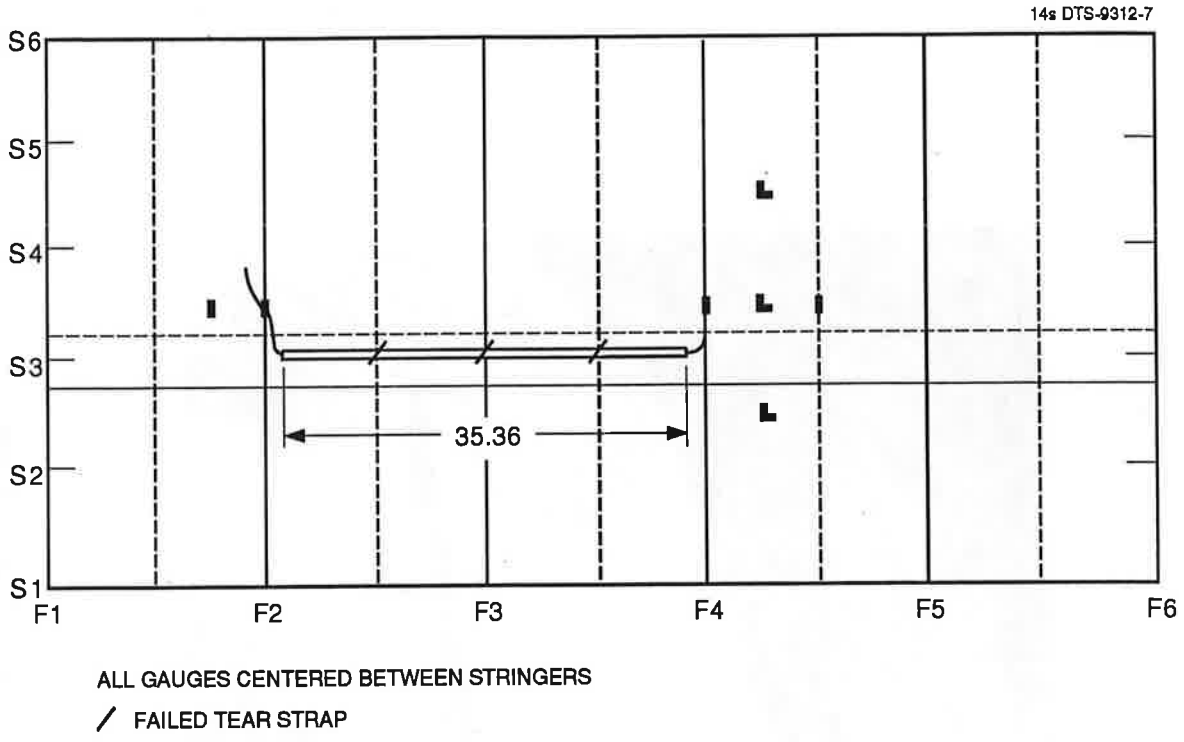

Figure 18. Panel 14 - After Fracture

4.4 Analysis of Residual Strength Tests

4.4.1 Loading Comparison

Strain gauge data recorded during failure testing indicate that all panels were comparably loaded. The five key gauge locations, plotted against panel pressure in Figures 22 through 26 and referenced to Figure 9, all show little scatter between the tests. Gauge locations 1 and 2 (Figures 22 and 23) show that the midbay hoop strains are equivalent in the first bay on either side of the lap joint. Further comparison of gauge locations 2 and 3 (Figures 23 and 24) show that these strains are equivalent in the first bay beyond either lead crack tip. Comparison of gauge locations 4 and 5 (Figures 25 and 26) show that the hoop strains are equivalent in the bays containing either lead crack tip. Based on these measurements, the seven panels were similarly loaded.

4.4.2 Panel Failure

Several panel failure modes could be considered for definition of the residual strength. These could include the onset of crack growth, the onset of fast crack growth, the failure of one or more tear straps, etc. For the following reasons, the onset of fast crack growth was identified as the indicator of panel residual strength. As was discussed previously, an incremental loading procedure was used for the test of Panel No. 10 and all subsequent tests as a result of the observation of stable crack growth in the tests of Panel Nos. 8 and 9. Therefore, with this incremental loading, the panel pressure which caused fast crack growth could be observed and held during testing. Further, while the onset of fast crack growth could be quantified in Panel Nos. 8 and 9, the initiating pressure was not held and thus an artificially high ultimate panel failure pressure was reached. The initial onset of crack growth was also not considered to be an acceptable failure criteria as crack propagation was observed to self arrest after initial growth when a constant pressure was held. From the crack propagation data of the incrementally loaded panels, it was determined that fast crack growth typically coincided with a total crack growth ($\Delta 2a$)) of 0.10 in. Therefore, the panel pressure which yields this crack propagation was defined as the failure pressure for comparison of all tests.

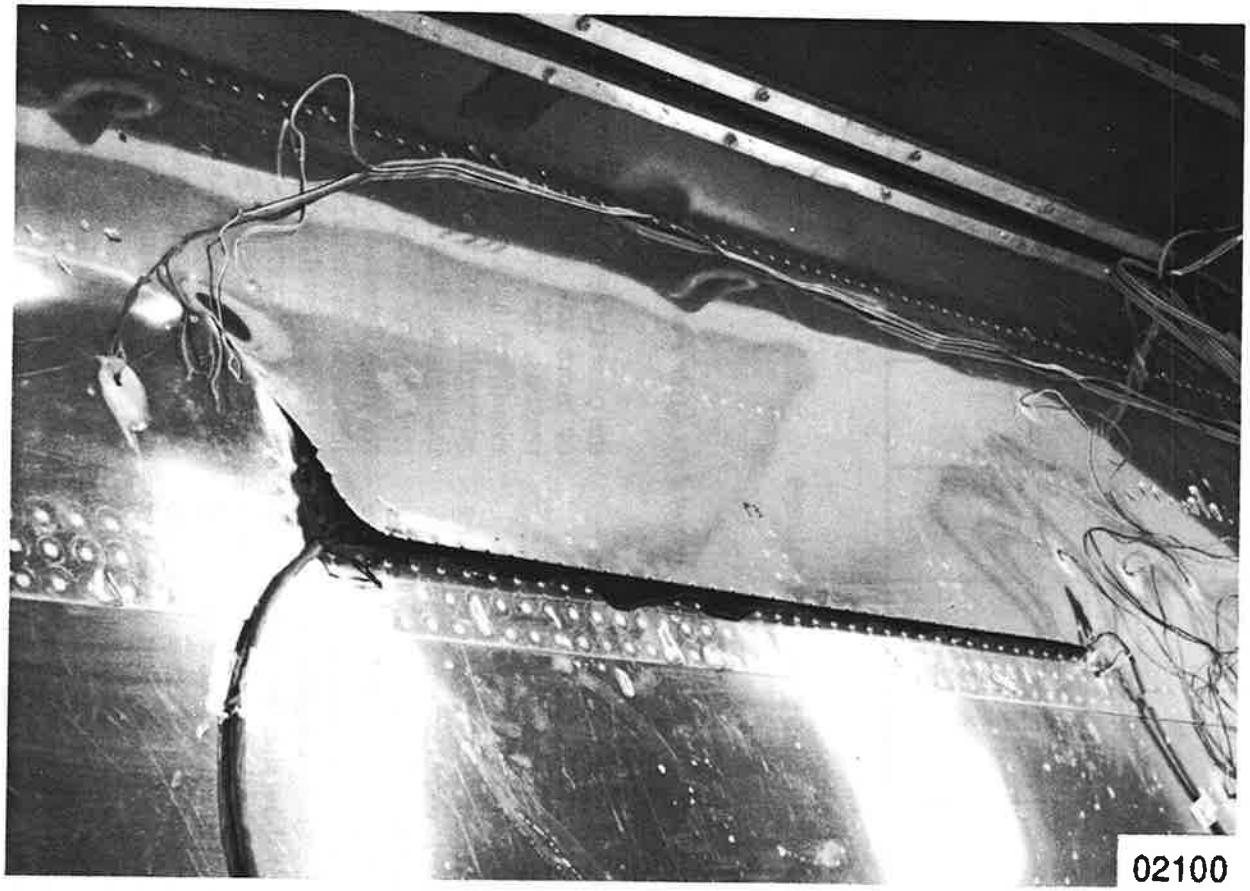

Figure 19. Panel 14: 35.36 in. Crack, No MSD - After Fracture

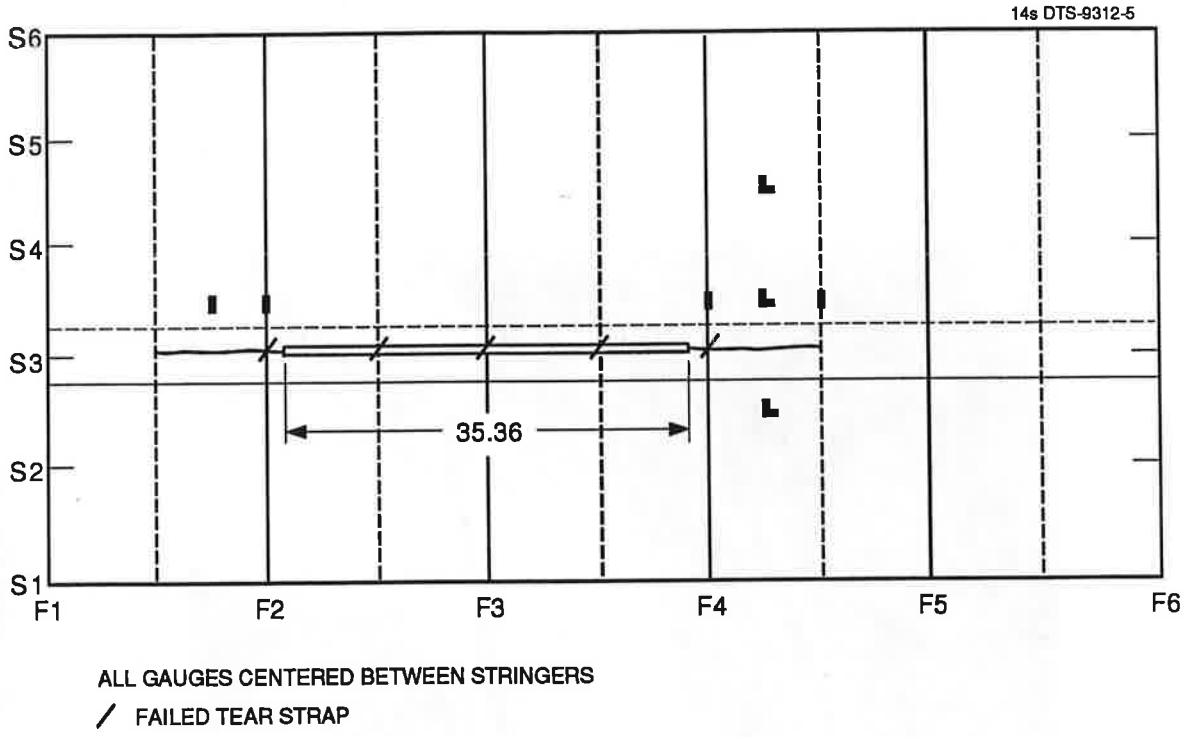

Figure 20. Panel 15 - After Fracture

The residual strengths (failure pressures) for the test panels were shown in Table 5. The relationship between failure pressure and lead crack length is shown in Figure 27. The strength reduction due to MSD can be related, by an elementary analysis, to the area of the first ligament beyond the lead crack tips. The net section areas for the with and without MSD conditions are shown in Figure 28. The area ratio of 0.88 compares well with the failure pressure ratios for the shorter lead cracks.

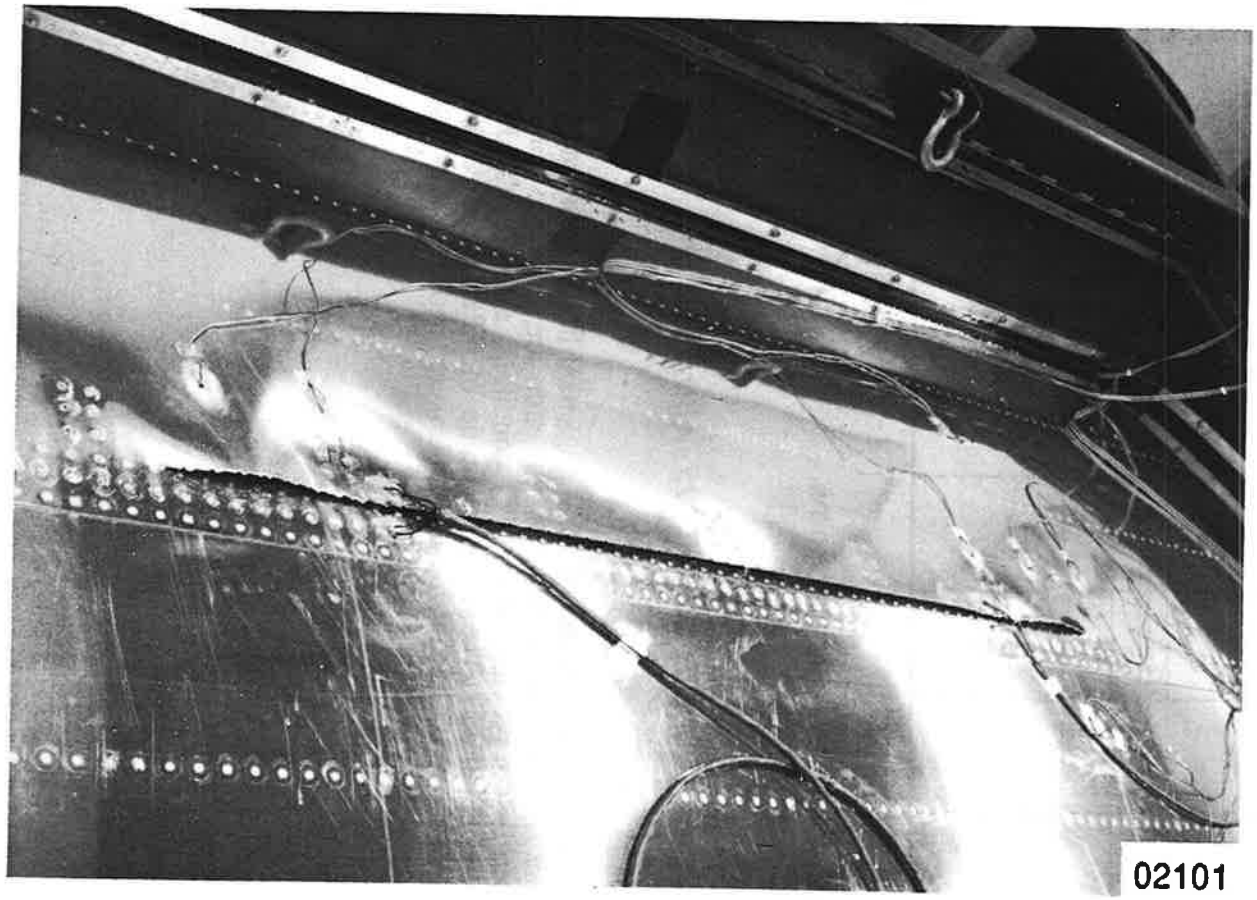

Figure 21. Panel 15: 35.36 in. Crack, No MSD - After Fracture

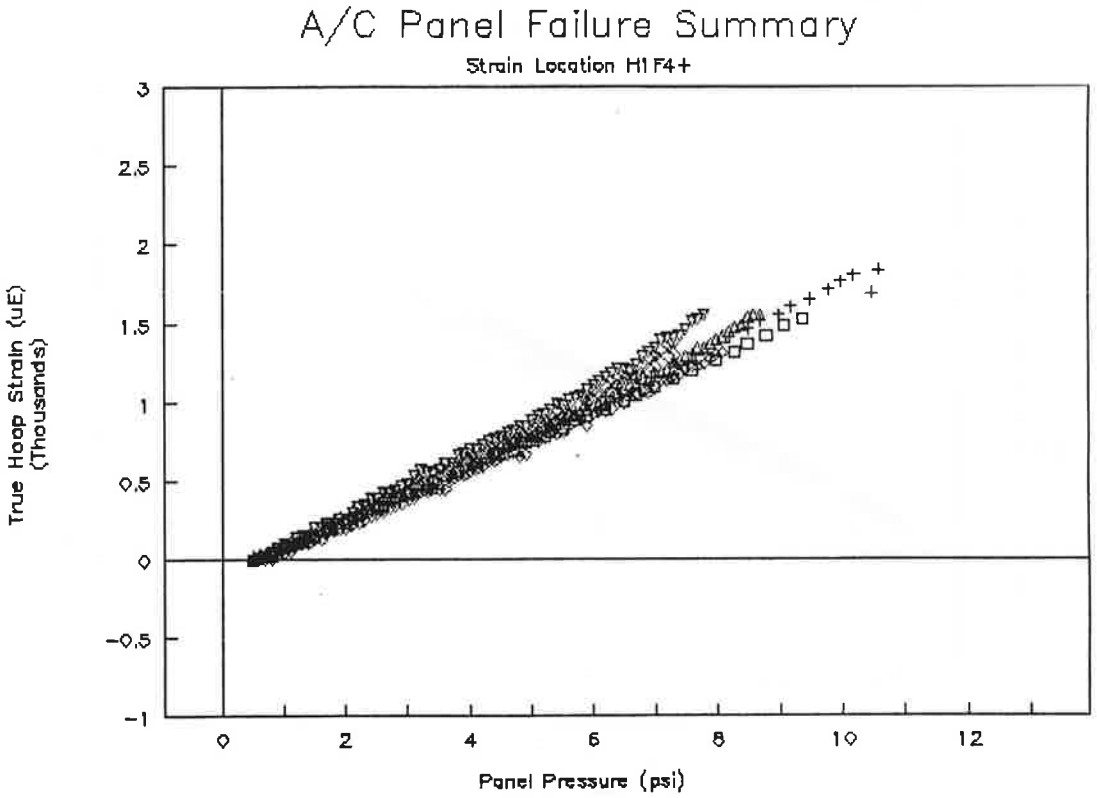

Figure 22. Panel Residual Strength Tests: Gauge No. 1

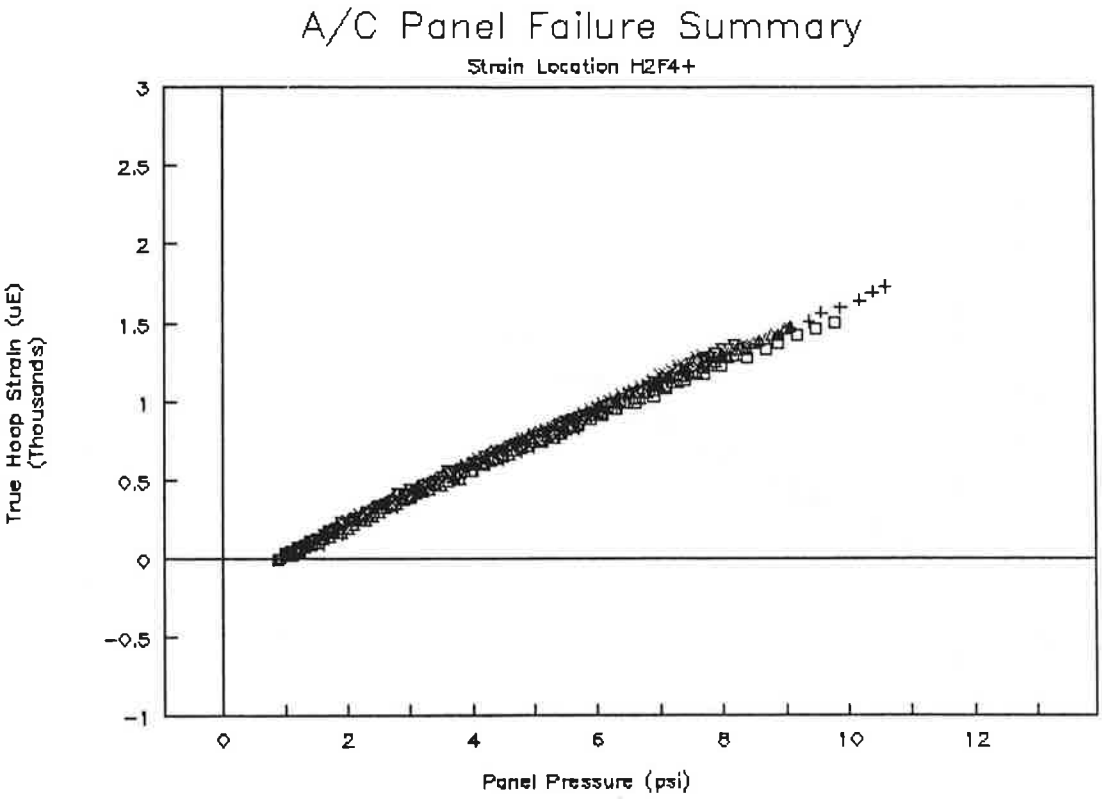

Figure 23. Panel Residual Strength Tests: Gauge No. 2

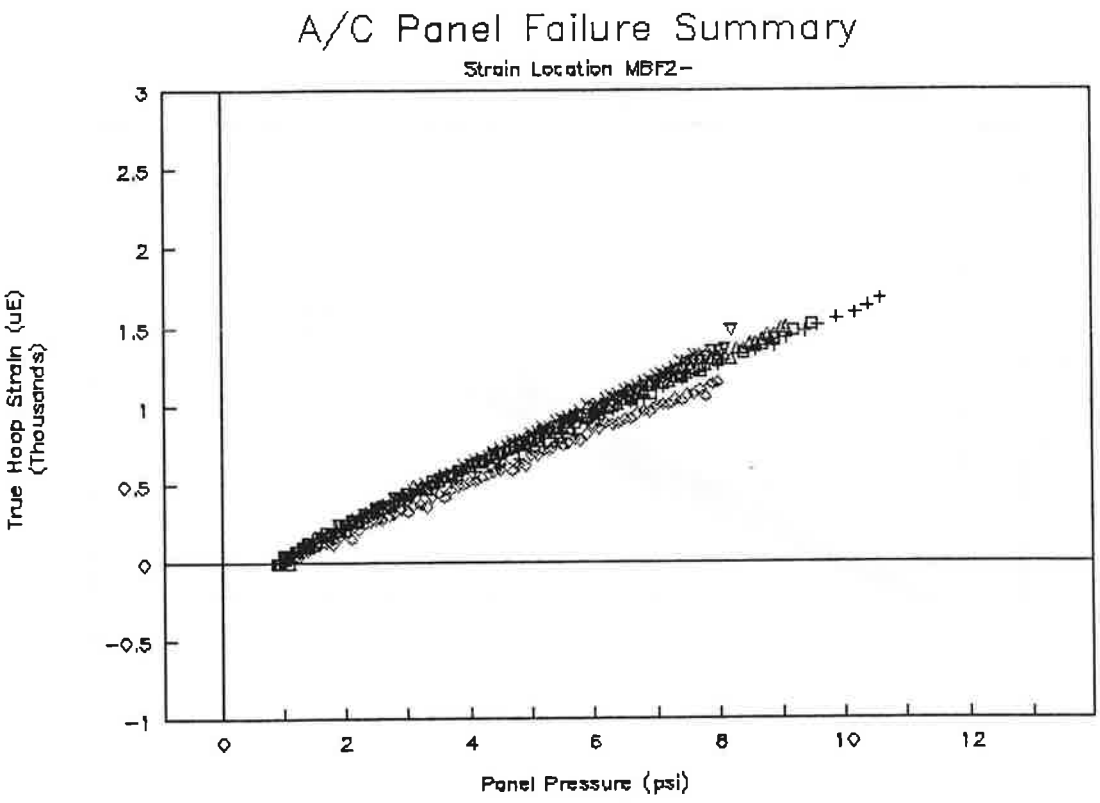

Figure 24. Panel Residual Strength Tests: Gauge No. 3

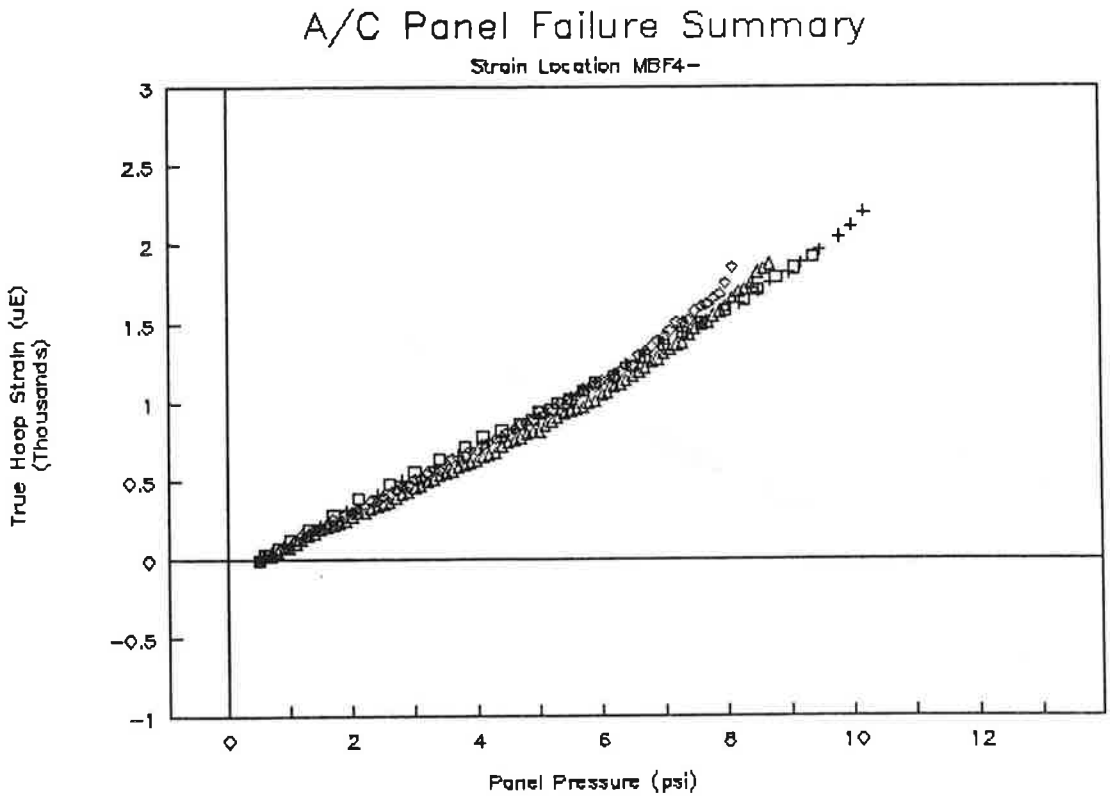

Figure 25. Panel Residual Strength Tests: Gauge No. 4

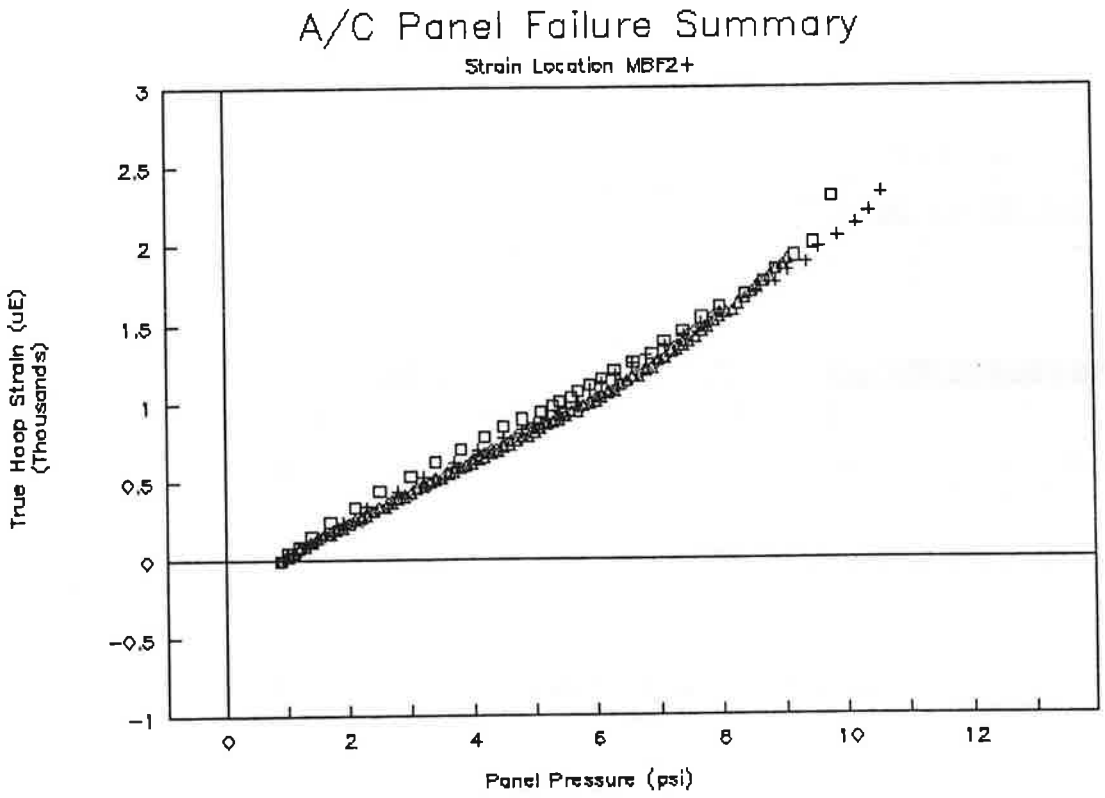

Figure 26. Panel Residual Strength Tests: Gauge No. 5

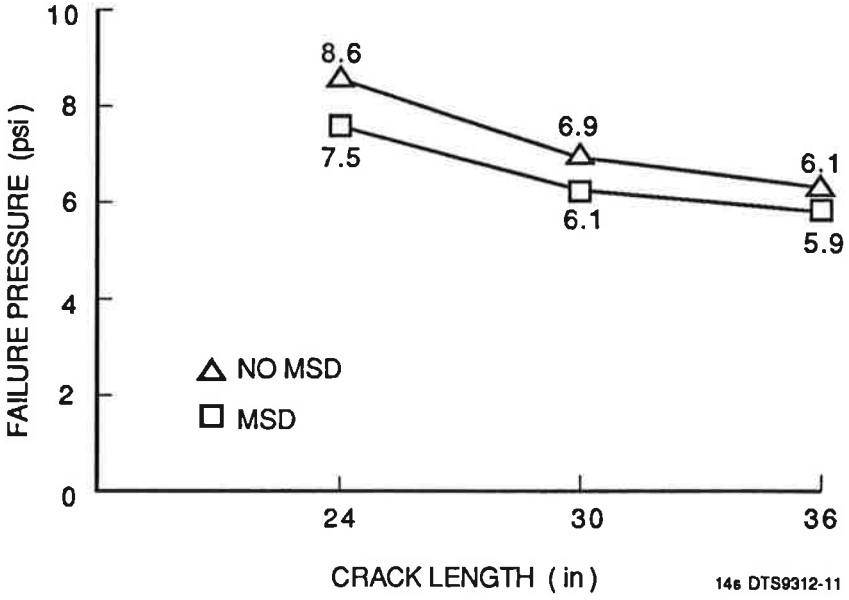

Figure 27. Panel Residual Strength

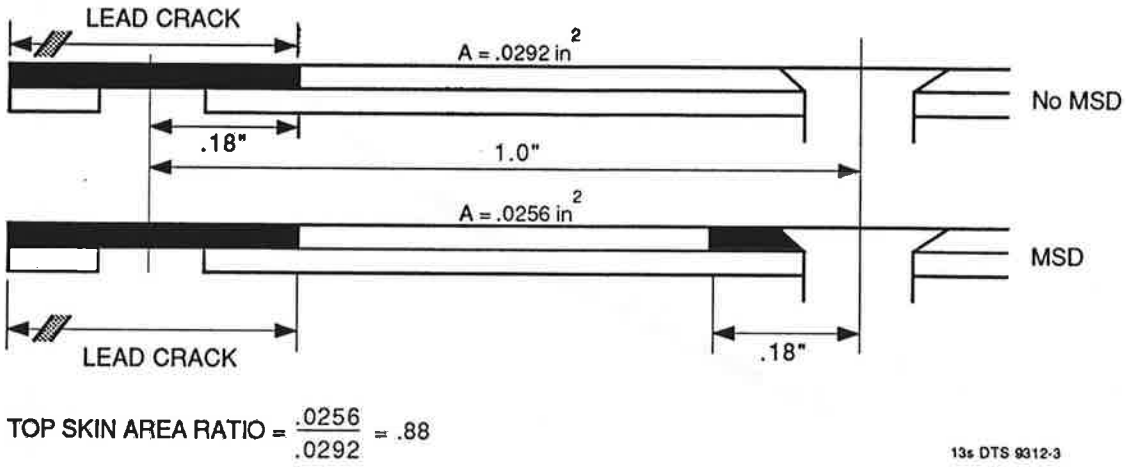

Figure 28. Crack Tip Ligament Net Section Areas

5. PANEL FATIGUE TEST

A high cycle fatigue test was performed on Panel 12 to study the formation and growth of Multiple Site Damage (MSD) in an initially undamaged panel. This test was also conducted to characterize the stress field throughout the panel. This test panel, as discussed in subsection 3.2, was fabricated with no initial mechanical damage and a completely unbonded lap joint.

5.1 Instrumentation

This test panel was heavily instrumented with a total of 41 strain gauges at the locations indicated in Figure 29. Several gauges were added during the initial static tests to more completely define both the membrane and bending stress distributions. In addition to the numerous strain gauges, applied panel pressures and loading system hydraulic pressures were measured with pressure transducers. The applied loads of the test machine were also output to the data acquisition system. Videotape provided a continuous record of the testing as the instrumentation was not continuously recorded throughout the duration of cycling.

5.2 Static Tests

The test panel was statically loaded to 9.5 psi several times prior to the beginning of fatigue cycling. As this was the first panel, tested under this program which did not have any initial mechanical damage, it provided the opportunity to characterize the panel stress distribution. In particular, the membrane and bending stresses across the lap joint were measured.

The hoop stress distribution between F3 and the tear strap between F3 and F4 is shown in Figure 30. These stress levels were recorded at midbay. Based on data from internal gauges, there is negligible bending at midbay and thus the top skin strain can be considered to be the membrane strain. The measurements are compared with data taken from tests of a full round fuselage structure (6).

The bending stress distribution across the lap joint is shown in Figure 31. Measurements taken from both the inner and outer skin surfaces indicated that the membrane stress in the hoop direction was consistently 14.2 Ksi at midbay. The distribution shown was measured midway between a frame and a tear strap. A positive bending stress defines a reduction in local panel radius of curvature and thus a higher outer surface stress. The figure shows that the bending is highest (~6 Ksi) at the lower row of rivets. This may be due in part to the fact that internal pressurization results in bending about the rivet line on the lower side of the lap joint and bending about the lower skin edge on the upper side of the lap joint. Characteristics unique to panel construction may contribute to this phenomenon.

5.3 Finite Element Analysis

A finite element analysis was conducted to study the resultant deformation of the panel sheets in the lap joint under internal pressure. Figure 32 shows the superimposed sheet geometry before and after the application of the internal pressure (8.5 psi). This gives a clear picture of the state of stress of the sheets. In an actual panel this type of physical deformation is not observed because the model does not account for the structural stiffeners.

A second finite analysis model was used to study the effect of introducing a restrained stringer at the middle rivet row. The polar moment of inertia of the stringer is very large in comparison to that of the lap joint. The stringer is also restrained by the frame at regular intervals. The deformed shape of the strengthened panel

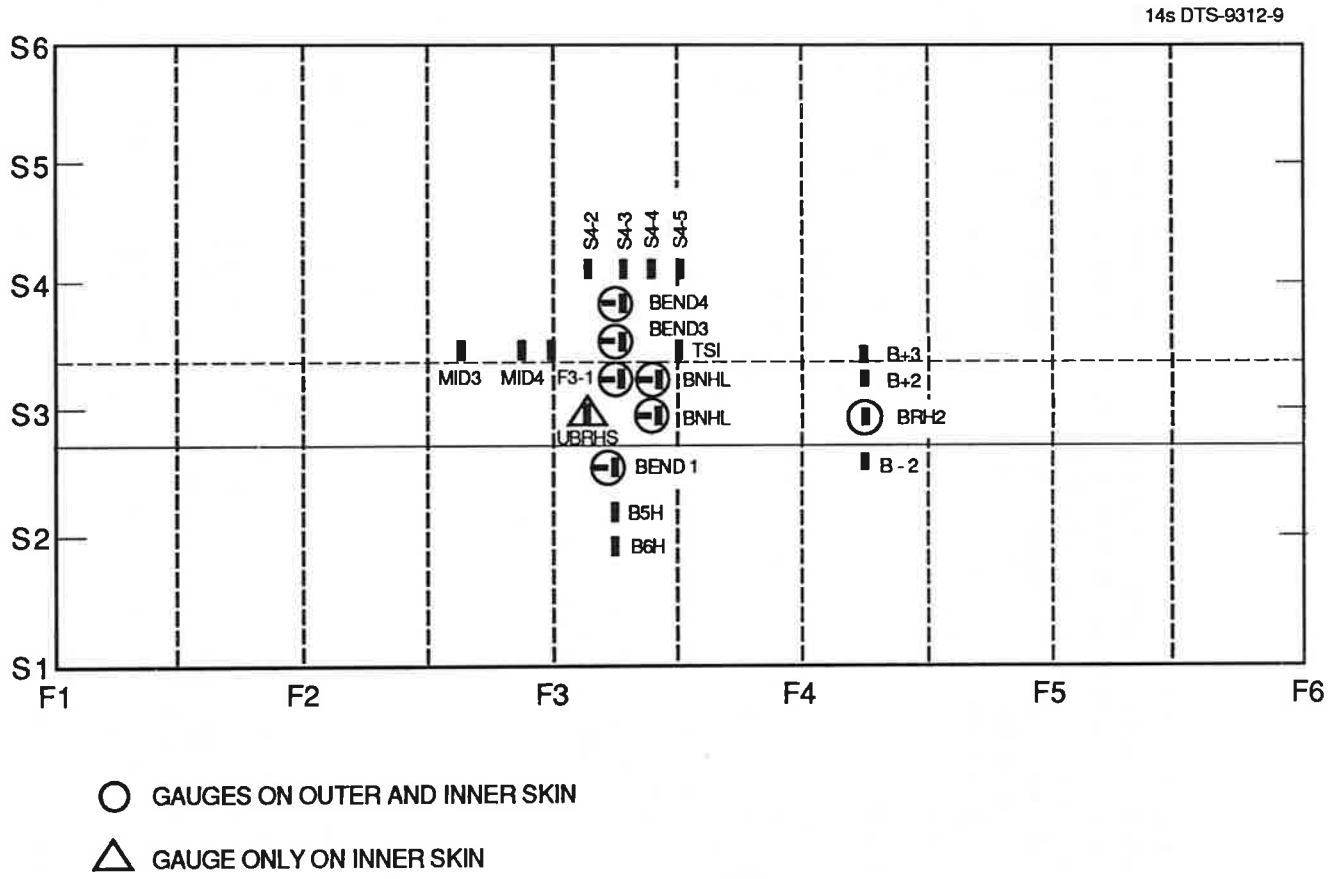

Figure 29. Panel 12 - Top, Outside

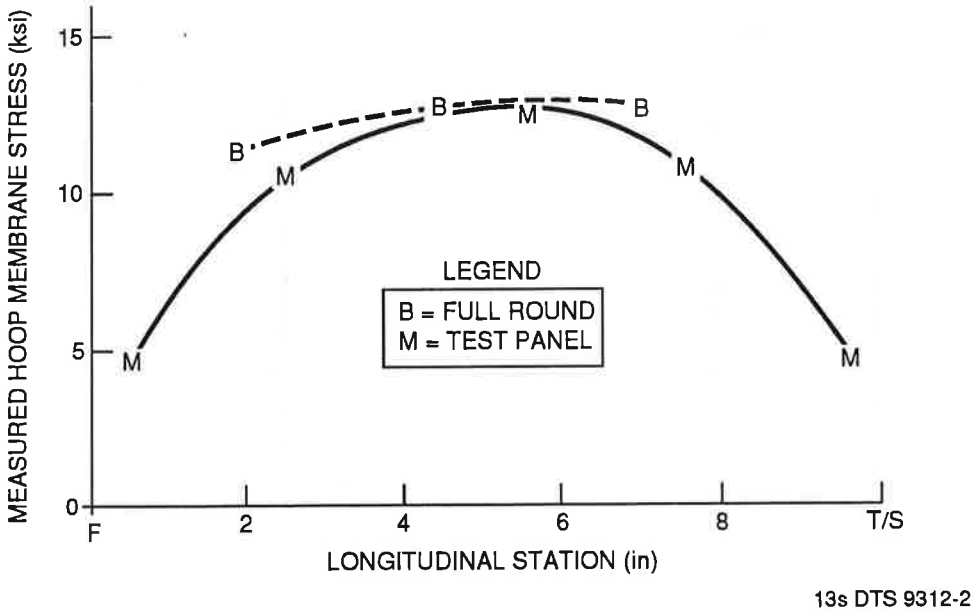

Figure 30. Hoop Stress Distribution in Panel 12

under internal pressure (8.5 psi) is compared with its undeformed shape in Figure 33.

These two idealized models qualitatively show the simplified state of stress in the lap joint vicinity. An actual panel assembly is much more complex than the finite element studies done above. The physical test results reflect this complex behavior of the test panel. The second model was used to calculate the membrane and bending stresses in the idealized panel. Figure 34 shows the comparison of the model results with the measured test data.

5.4 Fatigue Cycling

The panel was fatigue loaded to failure. Pressure cycling was applied at 0.2 Hz over a pressure range of 8.5 psi with a loading ratio of 0.11 (minimum pressure of 1 psi and maximum pressure of 9.5 psi). Static loading was applied at the beginning of each testing day and strains were measured to confirm consistent loading. Data were also collected during cycling to verify panel performance. Cyclic strain measurements confirmed, as with the Phase I tests, that the hoop and longitudinal loading were in phase. This phasing of strain and pressure measurements is shown in Figure 35. Panel radial deflection was also recorded at numerous locations throughout the panel. Figure 36 presents the radial deflection data at several longitudinal stations. As shown, the distributions are similar at each station except for F1 at the end of the panel where some edge effects are evident. This data also shows the most severe bending to be in the lower skin at the lower rivet line. This deflection distribution is thus in good agreement with the strain gauge data which was presented in Figure 31.

The progression of test events is summarized in Table 6. For convenience in identifying damage locations, the rivet stations were consecutively numbered from F1 to F6 as shown in Figure 37. Damage to the numerically ascending and descending sides of the rivet are designated "+" and "-" respectively.

The panel was cycled to 20,000 cycles, then removed for inspection. The panel was reinstalled and both inner and outer surfaces were inspected every 10,000 cycles. At 75,000 cycles, evidence

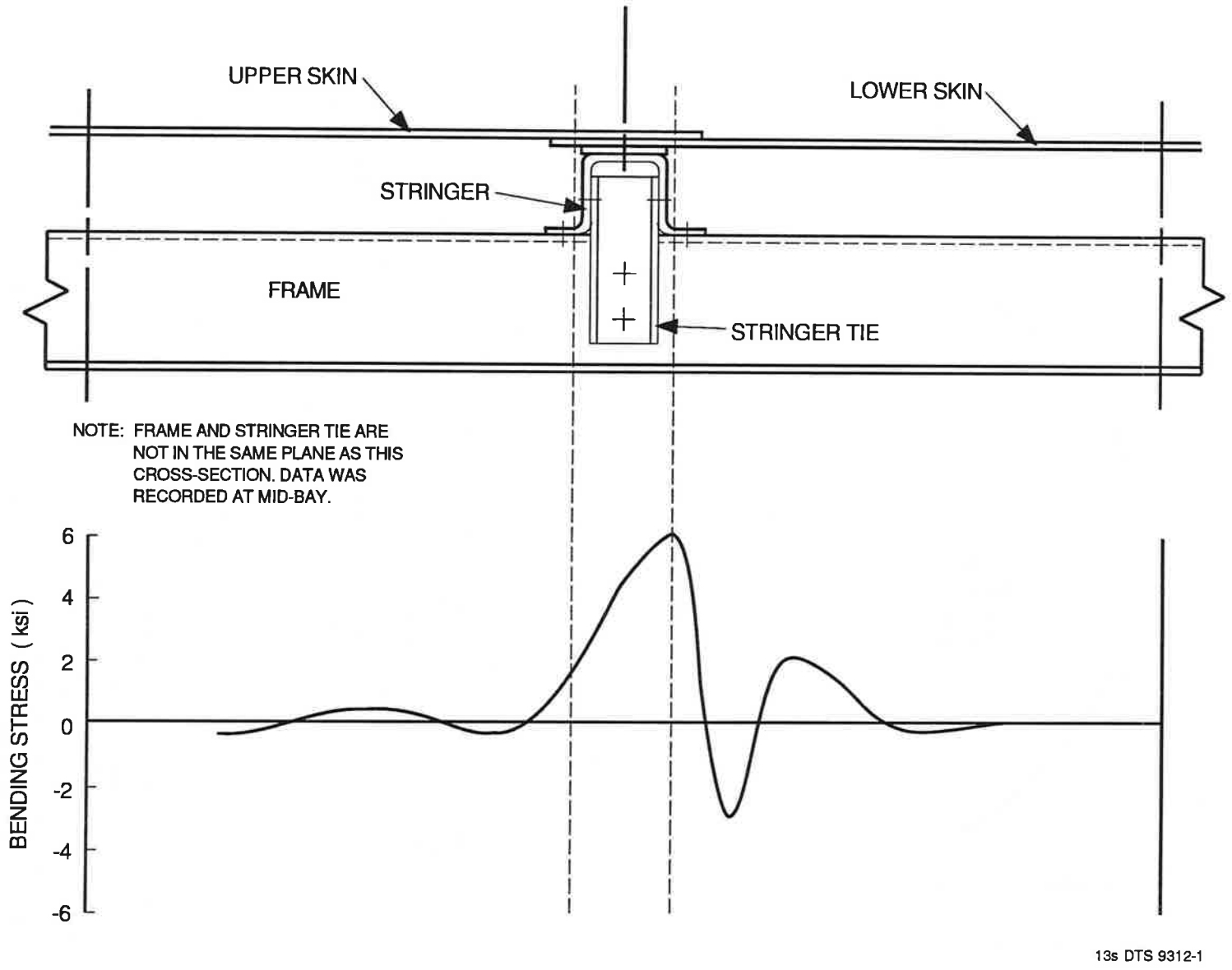

Figure 31. Bending Stress Distribtuion Across Lap Joint

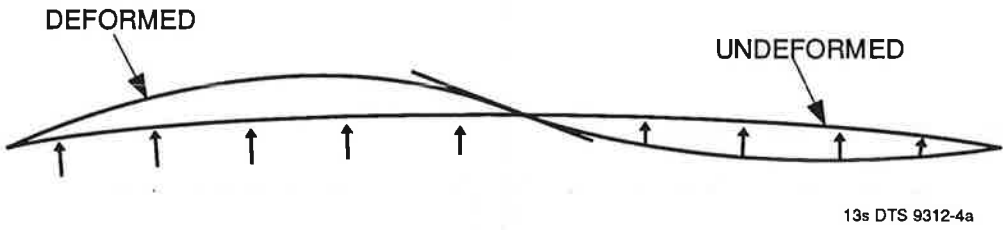

Figure 32. Deformation of an Unstiffened Lap Jointed Thin Shell Under Internal Pressure

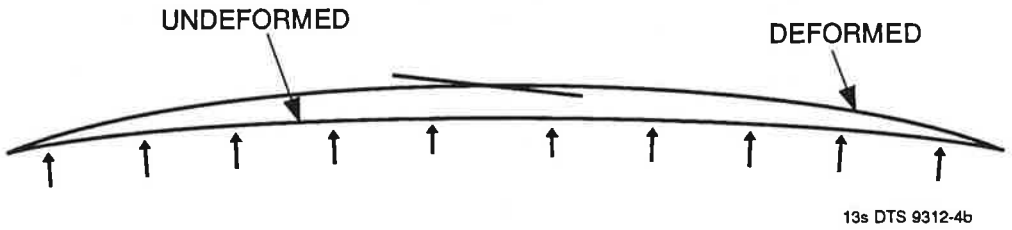

Figure 33. Deformation of a Stiffened Lap Jointed Thin Shell Under Internal Pressure

of bending damage was found on the underside of the panel along the lower rivet line. Cracks were also found at the longitudinal turnbuckle connection points. The panel was removed to repair turnbuckle connection points with the installation of bushings. Cycling resumed with an inspection interval of 5,000 cycles. At 96,193 cycles, a crack was detected on the upper rivet row. By 105,000 cycles, seven cracks were visible along the upper rivet row. At 114,571 cycles, lap joint leakage became pronounced. Upon inspection, link-up had occurred between rivets 35-37 on the lower rivet row. The panel fractured at 115,755 cycles. The failure occurred from rivets 22 through 51 on the lower rivet row, which ruptured the lower skin, as shown in Figures 38 through 40. No tear straps were broken.

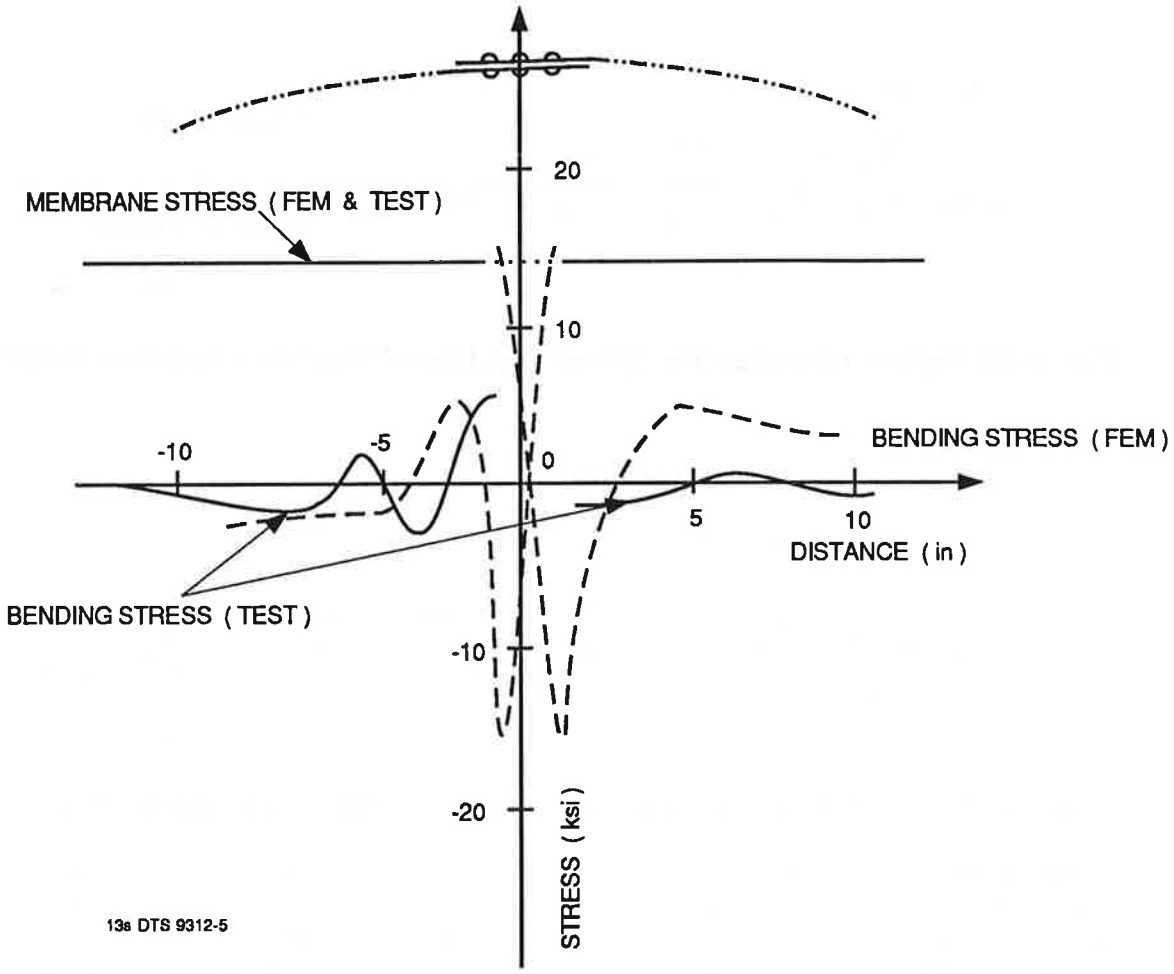

Figure 34. Membrane and Bending Stresses in the Lap Joint

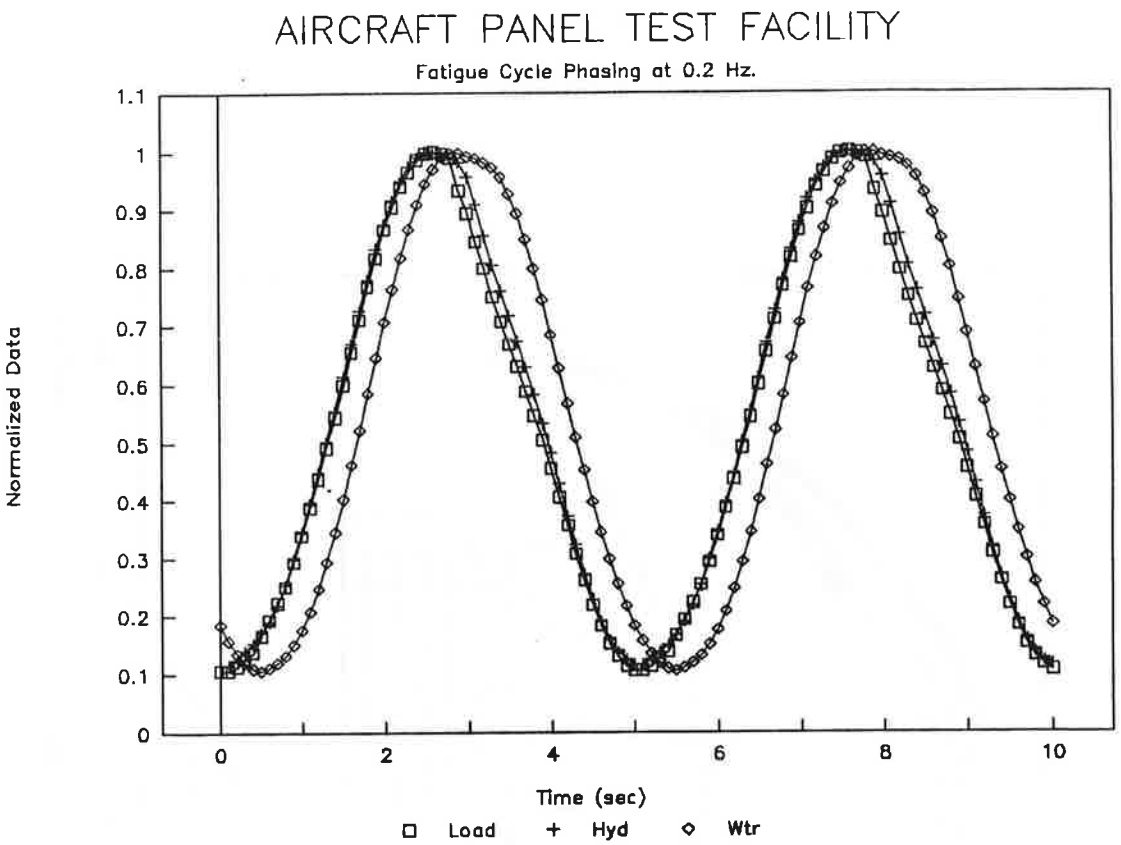

Figure 35. Pressure Cycling at 0.2 Hz

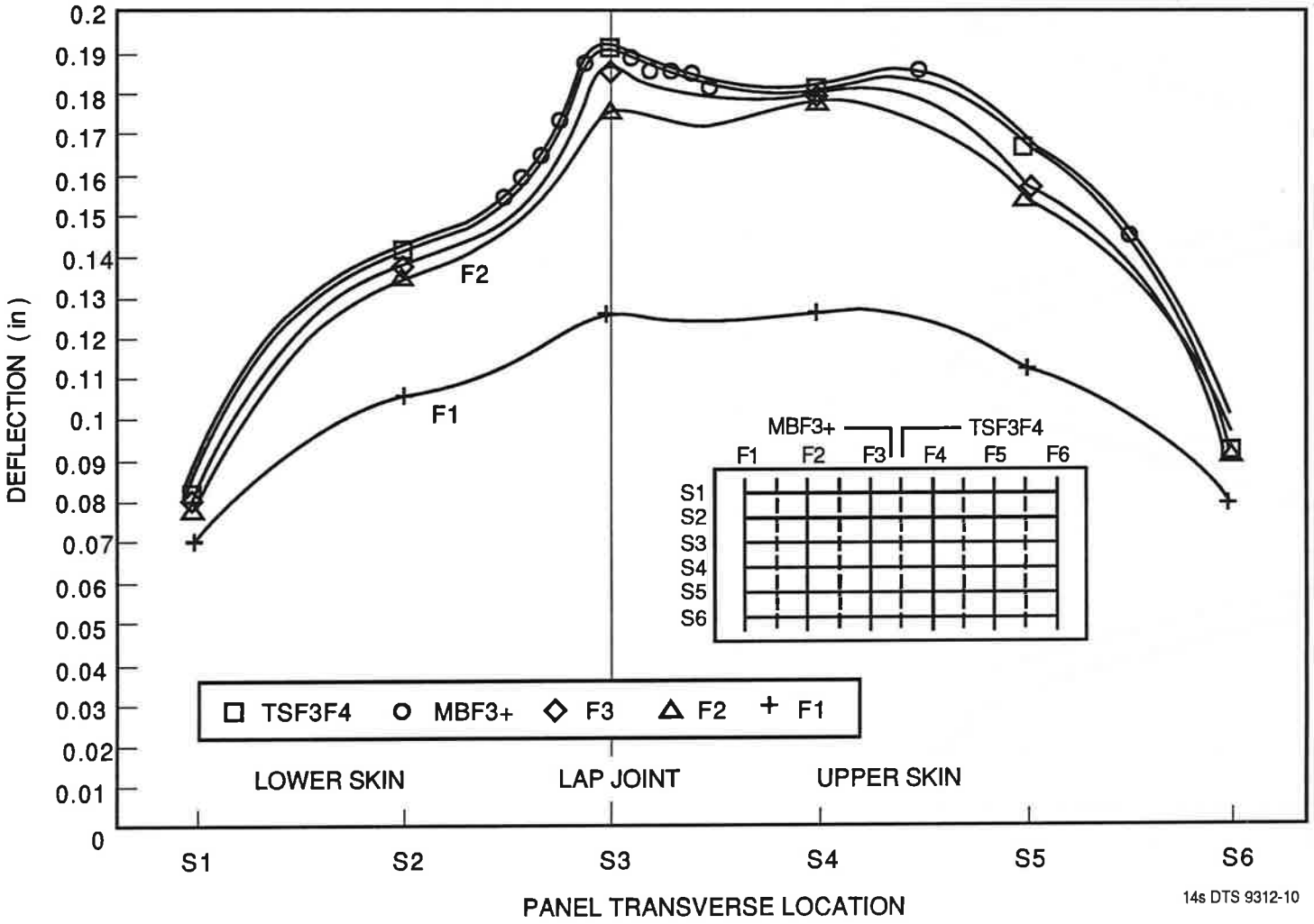

Figure 36. Cyclic Radial Deflection Distribution by Station in Panel 12

Table 6. Significant Fatigue Test Events

Inspection Interval (Cycle)	Upper Row Outer Skin	Lower Row Inner Skin
75,000	None	Microcracks at rivets 27, 28, 29
96,153	Skin crack at rivet 55+	No new damage
97,100	MSD at 55+, 59-	No new damage
98,782		Microcracks at rivets 26-30, 36-38, 48-50
100,239		26-30, 36-38, 48-50, 53
104,147	MSD at 55+, 59-, 71+, 72-	No new damage
105,397	Rivet Crack Length (in.) 52+ 0.060 55+ 0.080 59- 0.070 59+ 0.060 71- 0.050 71+ 0.060 72- 0.030 81+ 0.030	No new damage
113,816		Ligament broken between 36 and 37
114,571		35-37 broken
114,938		35-37, 27-28 broken
115,755	Rivet Crack Length (in.) 52+ 0.060 55+ 0.080 59- 0.070 59+ 0.060 71- 0.050 71+ 0.070 72- 0.060 81+ 0.050	Failure from rivet 22 to rivet 51

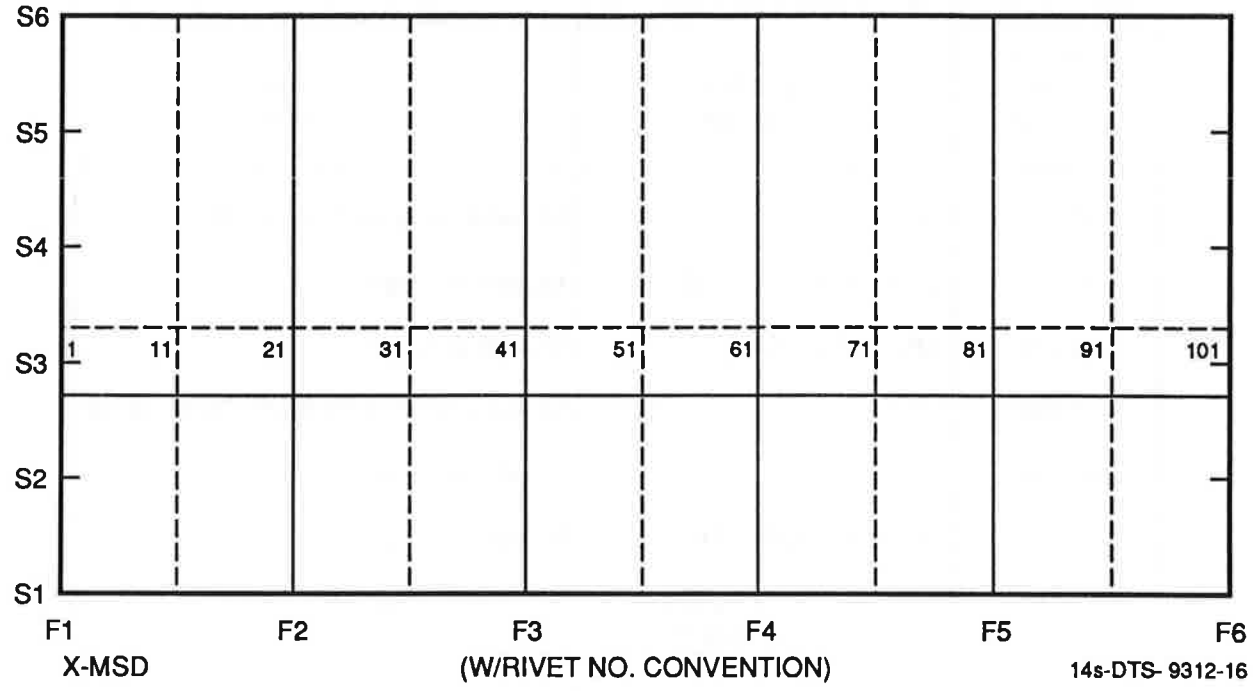

Figure 37. Test Panel No. 12 - Undamaged with Rivet Number Convention

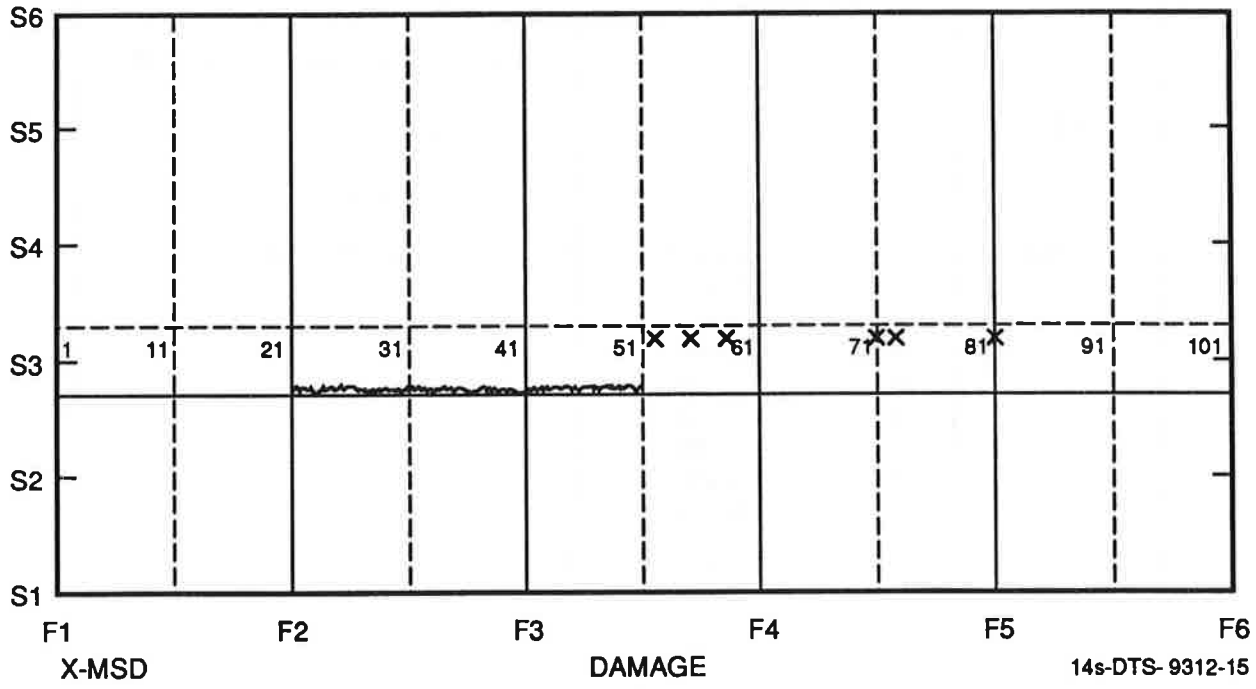

Figure 38. Test Panel No. 12 After Fracture

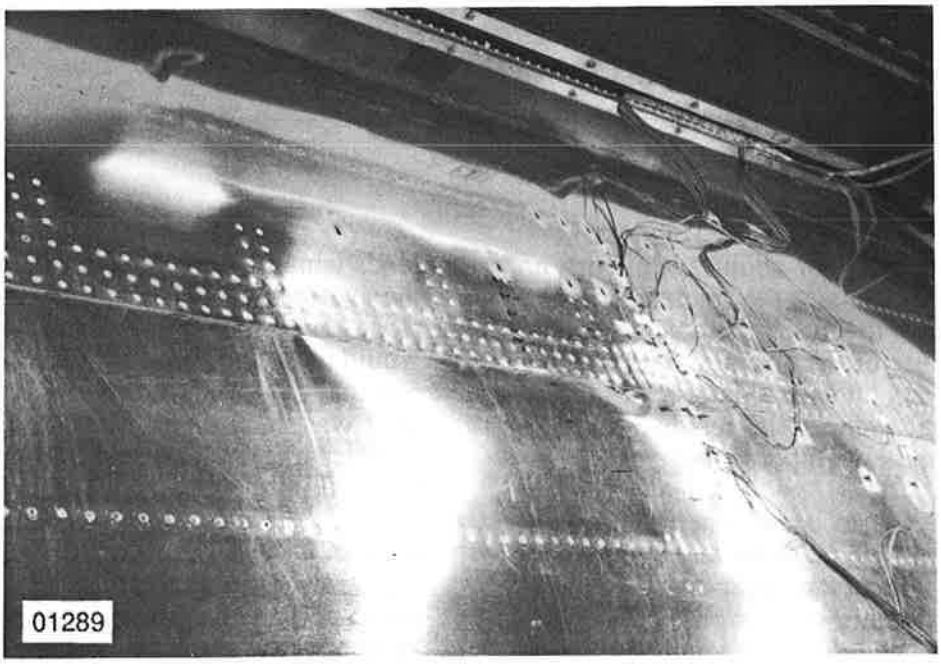

Figure 39. Panel 12: Outer Skin After Fracture

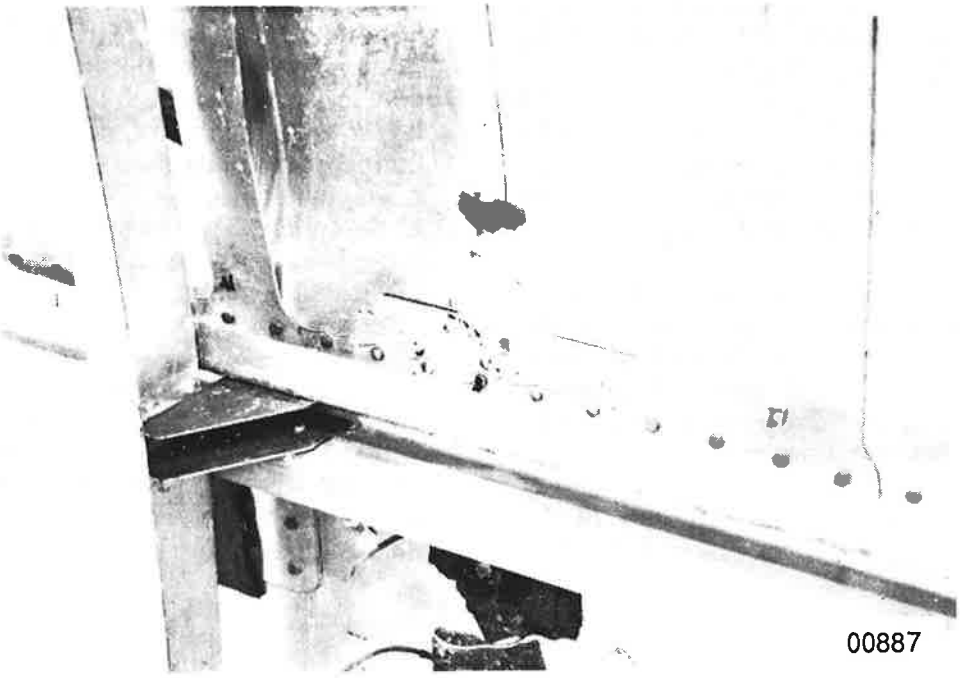

Figure 40. Panel 12: Inner Skin After Fracture

6. CONCLUSIONS AND RECOMMENDATIONS

- A lap splice crack of about 24 in. with no other damage reduces the fracture pressure approximately to the differential operational cabin pressure of the aircraft. MSD at five adjacent rivets on each side of a 24 in. lead crack further reduces the residual strength by approximately 15 percent (1 psi).

- Flapping seems to occur when the nearest MSD crack to the adjacent tear strap is less than one-half of the tear strap spacing (<5 in.). This is purely an empirical deduction from test data and although intuition supports it, additional testing may be required.

- Fracture is not always arrested at the first tear strap encountered by the crack. Although the fracture was always arrested by the following tear strap, this could be due to the drop in pressure in the test fixture. In real aircraft with sustained pressure, the cracks could continue to propagate.

- The presence of MSD in shorter lead cracks reduces the fracture pressure by a ratio roughly equal to the area ratio of the first ligaments beyond the lead crack tips.

- Under cyclic pressure fatigue loading MSD initiation in the critical upper rivet line of the lap splice may have been delayed due to the blunt countersink knife-edges. In some of the old aircraft, the sharp knife-edges could facilitate this initiation.

- MSD initiation in the critical row of the lower skin was accelerated by high bending loads which led to cracks along the edge of the rivet bucktails. The MSD did not emanate from the centerline of the rivet holes as would be indicative of tensile fatigue. Post-test analysis further supports this conclusion as it was determined that the cracks were initiated on the outer (mating) surface of the lower skin.

- Failure along the lower rivet line can apparently be contained by the structure as no tear straps failed during final fracture. However, the crack did not turn (flap) and thus no positive conclusion can be made as to its continued growth direction.

Recommendations

- Additional fatigue testing should be conducted to further investigate MSD initiation and link-up, simulating a sharp countersink knife-edge. The lap joint should be "reversed" in an effort to eliminate any non-representative lower skin bending which may occur due to the slight off center position of the splice. Two additional panels which incorporate these features have been fabricated and are available for this testing.

- Additional fatigue/fracture testing should be conducted on panels with shorter lead cracks with and without MSD. These panels should be cycled at operational pressure loads to investigate the mechanisms of failure and the residual fatigue lives.

7. REFERENCES

1. Samavedam, G., and D. Hoadley, "Fracture and Fatigue Strength Evaluation of Multiple Site Damaged Aircraft Fuselages - Curved Panel Testing and Analysis," Foster-Miller, Inc., May 1991.

2. Swift, T., "The Application of Fracture Mechanics in the Development of the DC-10 Fuselage," Fracture Mechanics of Aircraft Structures, AGARD-AG-176.

3. Pelloux, R., and D. Steul, "Failure Analysis Report, Foster-Miller Fatigue Test Panel." Department of Materials Science and Engineering, M.I.T., April 23, 1991.

4. FAA AC No. 43.13-1A "Acceptable Methods, Techniques, and Practices: Aircraft Inspection and Repair" (1972).

5. Gorenson, U., AATF R&D Committee Briefing, January 23, 1991, VNTSC.

6. Miller, M., "Hoop Stresses Adjacent to Stringer 4L Intact Structure," Boeing STRU-BY93B-P91-016.